

Bounds on Mosaic Number of Legendrian Knots

Margaret Kipe, Samantha Pezzimenti, Leif Schaumann,
Luc Ta, Wing Hong Tony Wong

October 11, 2024

Abstract

Mosaic tiles were first introduced by Lomonaco and Kauffman in 2008 to describe quantum knots, and have since been studied for their own right. Using a modified set of tiles, front projections of Legendrian knots can be built from mosaics as well. In this work, we compute lower bounds on the mosaic number of Legendrian knots in terms of their classical invariants. We also provide a class of examples that imply sharpness of these bounds in certain cases. An additional construction of Legendrian unknots provides an upper bound on the mosaic number of Legendrian unknots. We also adapt a result of Oh, Hong, Lee, and Lee to give an algorithm to compute the number of Legendrian link mosaics of any given size. Finally, we use a computer search to provide an updated census of known mosaic numbers for Legendrian knots, including all Legendrian knots whose mosaic number is 6 or less.

1 Introduction

1.1 Legendrian Knots

Legendrian knots are an important object of study in the field of contact topology. While a (smooth) **knot** is any embedding of a circle in \mathbb{R}^3 , a Legendrian knot has an extra geometric condition imposed by a contact structure.

In this paper, we will consider knots in the **standard contact structure on \mathbb{R}^3** , pictured in Figure 1. It is the plane field spanned by the vectors ∂_y and $\partial_x + y\partial_z$ at each point (x, y, z) in \mathbb{R}^3 , arising from the kernel of a differential one-form. Notice that the planes are horizontal along the x -axis and twist in the y -direction. They approach verticality, but never reach it. The intersection of these planes with the plane $y = y_0$ has a negative slope if $y_0 > 0$ and has a positive slope if $y_0 < 0$. The planes translate in the x and z direction, so all change occurs in the y -direction. One important feature of the standard contact structure is that no surface can be everywhere tangent to these planes. However, curves satisfying this property do exist and are called *Legendrian*. In particular, a **Legendrian knot (or link)** is a knot (or link) whose tangent space lies within the planes of the contact structure. For an intuitive introduction to Legendrian

knots, we refer the reader to [15]. For a more formal treatment, we refer the reader to [4].

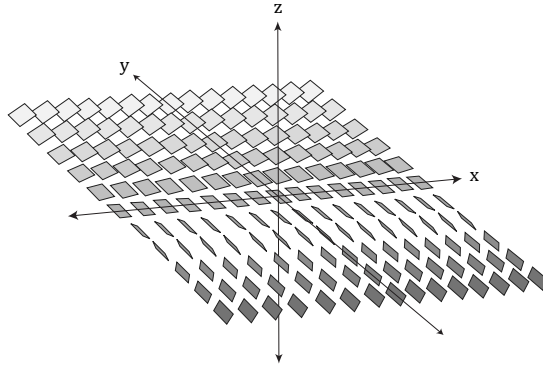


Figure 1: The standard contact structure on \mathbb{R}^3

Legendrian knots are commonly displayed in either their xy (Lagrangian) or xz (front) projections. In this paper, we will use the latter. Front projections of Legendrian knots have two key features that distinguish them from smooth knots: (1) since tangent lines can never be vertical, they have cusps in place of vertical tangencies; and (2) the direction of twisting ensures the strand with the more negative slope is the overstrand. Figure 2 shows a smooth positive trefoil and a Legendrian positive trefoil in its front projection. In this paper we will commonly refer to a “front projection of a Legendrian knot” as just a “Legendrian knot.”

For a given smooth knot type, there are infinitely many Legendrian knots of that type. One way to distinguish these are through their *classical invariants*—namely, the Thurston-Bennequin (tb) and rotation (rot) numbers. These invariants can be computed from an oriented front projection diagram. The **Thurston-Bennequin number** of a Legendrian knot Λ is computed by

$$tb(\Lambda) = P - N - \frac{1}{2}C,$$

where P is the number of positive crossings, N is the number of negative crossings, and C is the number of cusps in the diagram. (Note that the quantity



Figure 2: Smooth positive trefoil (left) and Legendrian positive trefoil (right).

$P - N$ is often called the **writhe** $w(\Lambda)$ of Λ , which is not an invariant.) The **rotation number** of Λ is

$$\text{rot}(\Lambda) = \frac{1}{2}(D - U),$$

where D is the number of downward pointing cusps and U is the number of upward pointing cusps. For certain knot classes, including unknots [3], torus knots [5], and certain twist knots [7], Legendrian knots are entirely classified by these classical invariants. It is common to organize this information into a “mountain range” like the ones in Figure 3. A mountain range is associated to a given smooth knot. Each dot represents a Legendrian knot with the specified classical invariants.

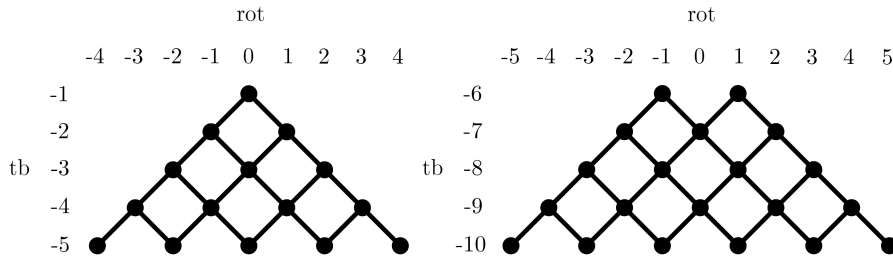


Figure 3: Mountain ranges of the Legendrian unknot (left) and Legendrian negative trefoil (right).

Each Legendrian knot represented in a mountain range can be obtained from an element higher up the mountain through a process called *stabilization*, pictured in Figure 4. From the front diagram, this can be viewed as adding a pair of cusps. A **positive** (respectively, **negative**) **stabilization** replaces an oriented strand with a pair of downward-oriented (respectively, upward-oriented) cusps. A Legendrian knot which can be obtained from another via stabilization is called *stabilized*. Note that a positive stabilization increases the rotation number by 1, while a negative stabilization decreases the rotation number by 1. Either stabilization decreases the Thurston-Bennequin invariant by 1. Also note that inserting a “twist” on an upward (respectively, downward) oriented cusp is equivalent to a positive (respectively, negative) stabilization.

1.2 Knot Mosaics

In 2008, Lomonaco and Kauffman [11] introduced a method of building knots using the mosaic tiles in Figure 5 as a means of describing quantum knots. An *n*-**mosaic** is an $n \times n$ array of tiles T_0, \dots, T_{10} , or equivalently, an $n \times n$ matrix whose entries are integers $0, \dots, 10$. An *n*-mosaic is **suitably connected** if the connection points of each tile coincide with connection points of contiguous tiles. An *n*-mosaic depicts a link if and only if it is suitably connected.

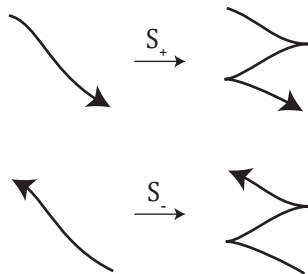


Figure 4: Positive and negative stabilization moves.

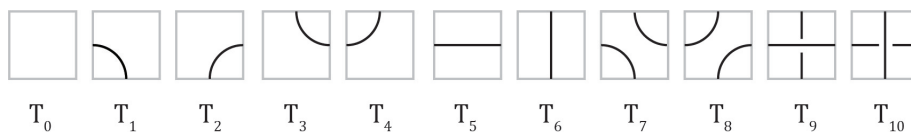


Figure 5: Original mosaic tiles to construct smooth knot mosaics.

Figure 6 shows a trefoil knot on a 4- and 5-mosaic. Although both are a valid mosaic representations of the trefoil, the 4-mosaic (right) appears to utilize the grid space more efficiently. To that end, the **mosaic number of a knot** K is the smallest integer n such that K can be represented on an n -mosaic. Indeed, it can be shown that the mosaic number of the trefoil knot is 4. The **inner board** of an n -mosaic is the $(n - 2)$ -submosaic consisting of all tiles except the boundary tiles. Since crossing tiles must be placed on the inner board (otherwise the boundary would contain a “loose end”), a 3-mosaic of a knot can have at most one crossing.

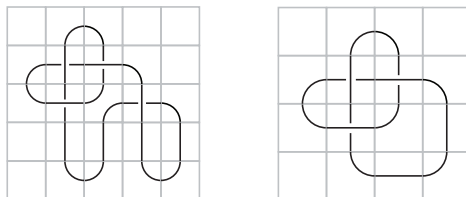


Figure 6: A trefoil knot on a 5-mosaic (left) and a 4-mosaic (right).

1.3 Legendrian Knot Mosaics

The remainder of this paper will focus on the intersection of knot mosaics and Legendrian knots. In 2022, Pezzimenti and Pandey [13] introduced the modified set of mosaic tiles in Figure 7 to construct front projections of Legendrian knots. Notice that the tile T_9 is eliminated since the strand with the more negative

slope must be the overstrand. A **Legendrian n -mosaic** is an array of the tiles in Figure 7 arranged in an $n \times n$ grid that has been rotated 45° counterclockwise. We refer to the (i, j) th position of the Legendrian mosaic as the (i, j) th position of the original grid.

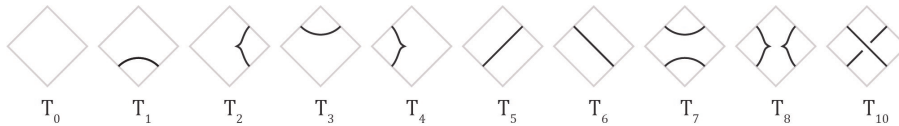


Figure 7: Legendrian mosaic tiles.

Figure 8 displays a Legendrian positive trefoil on a Legendrian 5-mosaic. Although the mosaic number $m(3_1)$ of the smooth trefoil is 4, it can be shown that if Λ represents a Legendrian positive trefoil with maximum Thurston-Bennequin invariant, its mosaic number $m(\Lambda)$ is indeed 5. Although the inner board contains 4 tiles, the restriction on crossing tiles means that there cannot exist a set of three alternating crossings.

Given a smooth knot type K , we also define the **Legendrian mosaic number** $m_L(K)$ of K to be the minimum mosaic number taken over all Legendrian representatives of K . For example, taking K to be the trefoil 3_1 , there exist positive and negative Legendrian trefoils that can be realized on Legendrian 5-mosaics, but no Legendrian trefoil can be realized on a Legendrian 4-mosaic. Thus, $m_L(3_1) = 5$. Note that the Legendrian mosaic number $m_L(K)$ is an invariant of *smooth* knots. On the other hand, we will consider the mosaic number $m(\Lambda)$ an invariant of *Legendrian* knots.

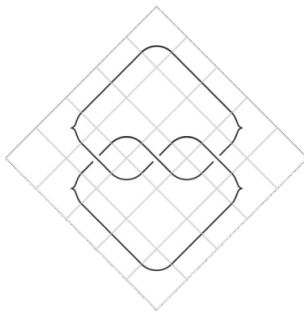


Figure 8: Legendrian positive trefoil on a 5-mosaic.

In [13], Pezzimenti and Pandey pose some open questions. One such question seeks bounds on the mosaic number of Legendrian knots via the classical invariants. In Section 2, we provide some bounds using both combinatorial and linear algebraic approaches. We also provide an infinite family of examples that prove sharpness of one of these bounds.

In Section 3, we provide an algorithm to construct mosaics of Legendrian unknots, which gives an upper bound on their mosaic number. This construction builds on the sequence in [13] of an infinite family of unknots that realize their mosaic numbers in non-reduced projections (i.e., projections with more than the minimum number of crossings).

In Section 4, we adapt the proof of Theorem 1 in [12] to give an algorithm to compute the number of $m \times n$ Legendrian link mosaics for all $m, n \in \mathbb{Z}^+$. In Appendix B, we give an implementation of this algorithm in Mathematica and our calculations for all $1 \leq n \leq m \leq 11$.

In Section 5, we describe a computer algorithm to produce all suitably connected Legendrian mosaics, and use it to compute the mosaic number of all Legendrian knots with mosaic number up to 6 via an exhaustive search. In Appendix C, we provide an updated census reflecting these results, which now extends to knots with up to 8 crossings. (The census in [13] previously included Legendrian unknots, and trefoils, up to size 5.) We highlight several instances of stabilized knots having a smaller mosaic number than their pre-stabilized counterparts, including a family of smooth knots whose Legendrian mosaic number is not realized by any Legendrian representatives with maximal Thurston-Bennequin number. This answers two more open questions from [13].

Finally, in Section 6, we suggest some further areas to explore related to our findings.

2 Lower Bounds from Classical Invariants

2.1 Oriented Legendrian Mosaic Tiles

In Appendix B of [11], Lomonaco and Kauffman consider all 29 possible combinations of orientations for strands on the 11 classical mosaic tiles in Figure 5. In this section, we similarly consider all 25 combinations of orientations for strands on the ten Legendrian mosaic tiles in Figure 7. These **oriented Legendrian mosaic tiles**, hereafter referred to as “oriented tiles,” are tabulated in Figure 9. In Sections 2.2 and 2.3, we will use these tiles to provide two lower bounds on the mosaic number of a Legendrian knot in terms of its classical invariants, applying both combinatorial and linear algebraic arguments.

We will begin by defining some useful functions based on these oriented tiles. Given an oriented Legendrian knot mosaic M , define $|M|_{R_i}$ as the number of times that the oriented tile R_i appears in M . Similarly, define $|M|_{T_i}$ as the number of times that any oriented (or unoriented) version of T_i appears in M .

For any oriented tile R_i , define $h(R_i) \in \{-2, -1, 0, 1, 2\}$ as the net horizontal movement of strands within R_i , measured in units of length $\sqrt{2}/2$ times the side length of a tile. Similarly, define $v(R_i) \in \{-2, -1, 0, 1, 2\}$ as the net vertical movement of strands within R_i . For example, Figure 10 shows the values of h and v for tiles R_3 , R_6 , and R_{22} . These functions are useful in finding restrictions of the possible valid combinations of tiles that can appear in a Legendrian knot mosaic, as shown in Proposition 1 below.

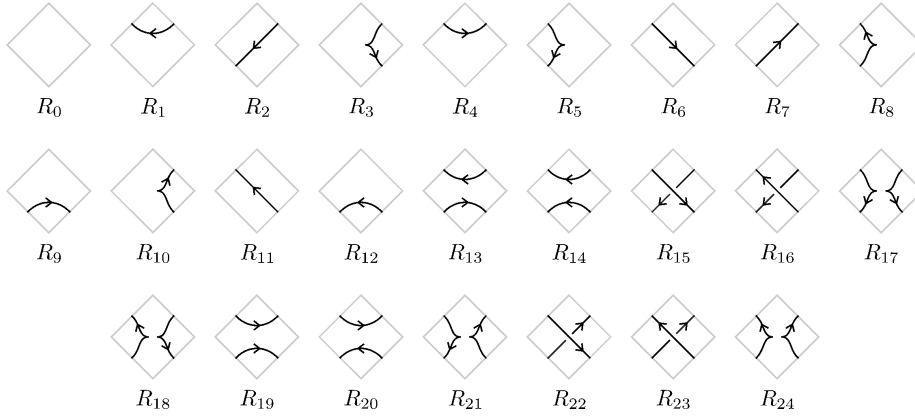


Figure 9: The 25 distinct oriented Legendrian knot mosaic tiles. (Note that the labeling is arbitrary).

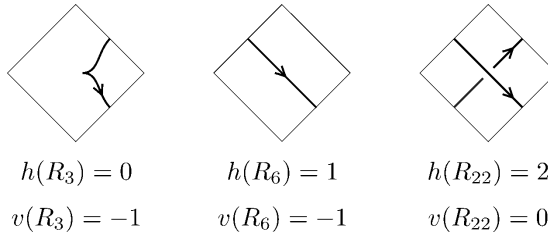


Figure 10: The values of the functions h and v for tiles R_3 , R_6 , and R_{22} .

Proposition 1. *Let M be an oriented knot mosaic representing a Legendrian knot Λ . Then*

$$\sum_{i=0}^{24} |M|_{R_i} h(R_i) = \sum_{i=0}^{24} |M|_{R_i} v(R_i) = 0.$$

Proof. When tracing the path of a knot on a mosaic, one passes through all of the strands exactly once, ending where the tracing began. This means that the net horizontal and vertical movement of all the tiles in a knot mosaic must sum to 0. \square

We will use the following consequence of this result to prove Theorem 1 in Section 2.2.

Lemma 1. *Let M be an oriented knot mosaic representing a Legendrian knot Λ . Let U and D denote the numbers of upward- and downward-oriented cusps in M , respectively, and let N denote the number of negative crossings. If $U \geq D$, then*

$$2|\text{rot}(\Lambda)| \leq 2N + |M|_{T_5} + |M|_{T_6}.$$

Proof. First, note that the quantity $D - U = 2 \operatorname{rot}(\Lambda)$ captures the signed vertical movement through cusp tiles while traversing the oriented knot mosaic. (Also note that U decreases the value of $2 \operatorname{rot}(\Lambda)$, while U increases the value of v , defined above.) Now, consider the following two sets of integers, which are disjoint:

$$S := \{3, 5, 8, 10, 17, 18, 21, 24\}, \quad S' := \{2, 6, 7, 11, 15, 23\}.$$

By Figure 9, an oriented tile R_i contains a cusp if and only if $i \in S$. Therefore, our characterization of the quantity $2 \operatorname{rot}(\Lambda)$ may be reformulated as the following equation:

$$2 \operatorname{rot}(\Lambda) = - \sum_{i \in S} |M|_{R_i} v(R_i).$$

It follows from Proposition 1 that

$$2 \operatorname{rot}(\Lambda) = \sum_{0 \leq i \leq 24, i \notin S} |M|_{R_i} v(R_i). \quad (1)$$

It is also evident from Figure 9 that for a given R_i with $i \notin S$ (i.e., R_i containing no cusps), then $i \in \{2, 6, 15\}$ if and only if $v(R_i) < 0$ (i.e., every strand in R_i moves downward and $i \neq 0$). Since $\{2, 6, 15\} \subset S'$, it follows that

$$\sum_{0 \leq i \leq 24, i \notin S} |M|_{R_i} v(R_i) \geq \sum_{i \in S'} |M|_{R_i} v(R_i). \quad (2)$$

Also, note that $i \in S'$ if and only if R_i either contains a negative crossing (in which case $v(R_i) = \pm 2$) or is an oriented T_5 or T_6 tile (in which case $v(R_i) = \pm 1$). Therefore,

$$- \sum_{i \in S'} |M|_{R_i} v(R_i) \leq 2N + |M|_{T_5} + |M|_{T_6}. \quad (3)$$

Now, our assumption that $U \geq D$ implies that $2 \operatorname{rot}(\Lambda) \leq 0$, or equivalently, $2|\operatorname{rot}(\Lambda)| = -2 \operatorname{rot}(\Lambda)$. Combining this equality with (1) yields

$$\begin{aligned} 2|\operatorname{rot}(\Lambda)| &= - \sum_{0 \leq i \leq 24, i \notin S} |M|_{R_i} v(R_i) \\ &\leq - \sum_{i \in S'} |M|_{R_i} v(R_i) && \text{by (2)} \\ &\leq 2N + |M|_{T_5} + |M|_{T_6}, && \text{by (3)} \end{aligned}$$

as desired. □

2.2 A Combinatorial Approach

In this section, we provide two lower bounds for the mosaic number of a Legendrian knot in terms of its classical invariants via combinatorial arguments. The

first lower bound, stated in Theorem 1 below, is most effective when the value of the quantity

$$k := |\text{rot}(\Lambda)| + \text{tb}(\Lambda)$$

is sufficiently high. The proof relies on manipulating inequalities involving k , the number of positive and negative crossings, and the number of upward- and downward-oriented cusps of an oriented Legendrian knot mosaic.

Theorem 1. *If Λ is a Legendrian knot and $4|\text{rot}(\Lambda)| + \text{tb}(\Lambda) \geq 0$, then*

$$m(\Lambda) \geq \left\lceil \sqrt{4|\text{rot}(\Lambda)| + \text{tb}(\Lambda)} \right\rceil.$$

Proof. Suppose a Legendrian knot Λ can be represented by an n -mosaic M . We will show that $n \geq \sqrt{3|\text{rot}(\Lambda)| + k}$. For the particular front projection of Λ represented in M , let U and D denote the numbers of upward- and downward-oriented cusps, respectively, and let P and N denote the numbers of positive and negative crossings, respectively.

Since $\text{rot}(\Lambda) = \frac{1}{2}(D - U)$, orientation only affects the sign of $\text{rot}(\Lambda)$. Without loss of generality, choose an orientation such that $U \geq D$. Since $D \geq 0$, this inequality implies $U \geq |D - U| = 2|\text{rot}(\Lambda)|$. Then, by definition,

$$\begin{aligned} \text{tb}(\Lambda) &= P - N - \frac{1}{2}(D + U) \\ &= P - N - \frac{1}{2}(D - U) - U \\ &= P - N - \text{rot}(\Lambda) - U \\ &\leq P - N + |\text{rot}(\Lambda)| - 2|\text{rot}(\Lambda)| \\ &= P - N - |\text{rot}(\Lambda)|. \end{aligned}$$

Substituting $\text{tb}(\Lambda) = k - |\text{rot}(\Lambda)|$ yields $k \leq P - N$, or,

$$P \geq k + N. \tag{4}$$

Now, let $c := \sum_{i \in \{2,4,8\}} |M|_{T_i}$ and observe that c is the number of tiles in M that contain cusps. Our earlier remark that $U \geq 2|\text{rot}(\Lambda)|$ implies

$$c \geq \frac{1}{2}U \geq |\text{rot}(\Lambda)|.$$

We can also consider the number of tiles in M that do not contain cusps:

$$\begin{aligned} n^2 - c &\geq P + N + |M|_{T_5} + |M|_{T_6} \\ &\geq k + 2N + |M|_{T_5} + |M|_{T_6} && \text{by (4)} \\ &\geq k + 2|\text{rot}(\Lambda)|. && \text{by Lemma 1} \end{aligned}$$

Hence,

$$n^2 \geq |\text{rot}(\Lambda)| + k + 2|\text{rot}(\Lambda)|.$$

Solving for n completes the proof. \square

Since the bound in Theorem 1 increases as $k = |\text{rot}(\Lambda)| + \text{tb}(\Lambda)$ increases, it is most effective for Legendrian knots on the “outermost boundary” of the mountain range of its smooth knot type. For example, consider the mountain range of Legendrian unknots (Figure 3, left). For every Legendrian unknot Λ on the outermost boundary of the mountain range, we have $k = -1$. Thus, Theorem 1 tells us, for example, that any such unknot with $|\text{rot}(\Lambda)| \geq 4, 6, \text{ or } 9$ satisfies

$$m(\Lambda) \geq \left\lceil \sqrt{3|\text{rot}(\Lambda)| + k} \right\rceil = \left\lceil \sqrt{3|\text{rot}(\Lambda)| - 1} \right\rceil = 4, 5, \text{ or } 6,$$

respectively. Our computational results in Figure C.1 suggest that these bounds are not sharp. Nevertheless, the linear algebraic argument used to prove Theorem 4 in Section 2.3 replicates the bound in Theorem 1. This suggests that this bound cannot be significantly improved without considering the geometric properties of Legendrian knot mosaics.

For all Legendrian unknots not on the outermost boundary of the mountain range, we have $k < -1$, making the bound in Theorem 1 less useful. This issue motivates the bound in Theorem 2 below. This bound is usually more powerful than the one in Theorem 1, and it is based solely on $\text{tb}(\Lambda)$. The proof takes an extremal approach by considering every possible way the tiles in the boundary and the inner board can contribute to the Thurston-Bennequin invariant of a Legendrian knot. We also employ the observation in Propositions 3.5 and 3.6 of [13] that a mosaic diagram of a Legendrian link containing b tiles in its outer boundary can have at most $b/2$ cusps in its outer boundary.

Theorem 2. *If Λ is a Legendrian knot with negative Thurston-Bennequin number, then*

$$m(\Lambda) \geq \left\lceil \sqrt{-\text{tb}(\Lambda) - \frac{3}{4} + \frac{3}{2}} \right\rceil.$$

Proof. Consider a Legendrian n -mosaic of Λ . Since none of the $4n - 4$ boundary tiles can contain crossings, the only way boundary tiles can contribute to $\text{tb}(\Lambda)$ is by having cusps. Since these tiles contain at most $(4n - 4)/2 = 2n - 2$ cusps, they collectively contribute $-(n - 1)$ or more to $\text{tb}(\Lambda)$.

Now, consider the $(n - 2)^2$ tiles in the inner board. Each may contain either a crossing (contributing -1 or 1 to $\text{tb}(\Lambda)$), a cusp (contributing $-1/2$ to $\text{tb}(\Lambda)$), or neither (contributing 0 to $\text{tb}(\Lambda)$). In other words, each tile in the inner board contributes -1 or more to $\text{tb}(\Lambda)$, so they collectively contribute $-(n - 2)^2$ or more to $\text{tb}(\Lambda)$. Altogether,

$$\text{tb}(\Lambda) \geq -(n - 2)^2 - (n - 1),$$

and thus,

$$-\text{tb}(\Lambda) \leq n^2 - 3n + 3 = \left(n - \frac{3}{2}\right)^2 + \frac{3}{4}.$$

Solving for n achieves the desired inequality. \square

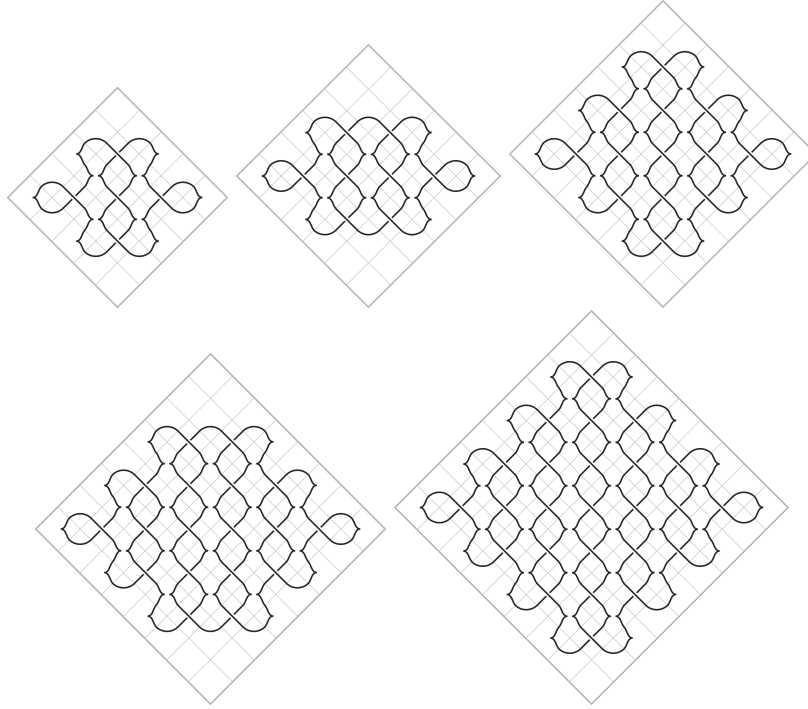


Figure 11: Crab buckets $\beta_5, \beta_6, \dots, \beta_9$.

The bound in Theorem 2 is sharp in infinitely many cases; in fact, it is attained by Legendrian representatives of infinitely many distinct smooth knot types. To show this, we construct an infinite sequence of Legendrian knots β_n , for $n \geq 5$ that each attain this bound. We call this sequence the sequence of *crab buckets* and refer to each β_n as the *n*th *crab bucket*. (See Section 6 for an explanation of the inspiration for this name.) Figure 11 depicts the first five crab buckets β_5, \dots, β_9 . For all $n \geq 5$, the *n*th crab bucket β_n can be constructed on a Legendrian *n*-mosaic as follows:

1. Starting with the tile in position $(2, 2)$, add as many nonadjacent T_{10} tiles into the inner board as possible.
2. If n is even, then add T_1 to the tile in position $(2, n - 1)$ and T_3 to the tile in position $(n - 1, 2)$.
3. Fill all remaining empty tiles in the inner board with T_8 .
4. Add T_1, T_2, T_3 , and T_4 tiles to the outer boundary of the mosaic to form a knot. (Note that there is only one way to do this due to the restricted movement of the strands connecting to the T_{10} tile in position $(2, 2)$, cf. the *twofold rule* stated in Section 2 of [12].)

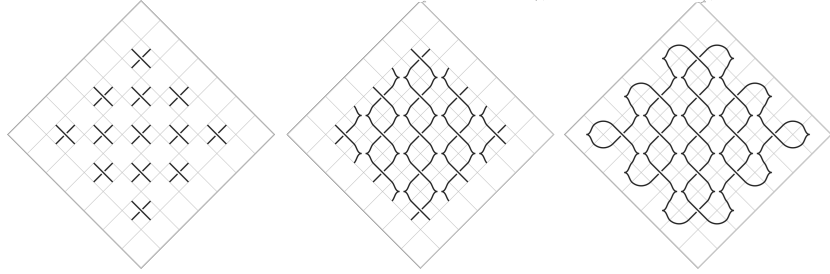


Figure 12: The construction of β_7 .

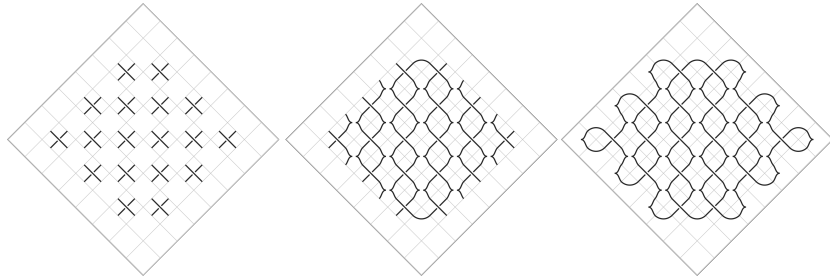


Figure 13: The construction of β_8 .

The steps of this construction in the odd and even cases are illustrated in Figures 12 and 13, respectively.

Recall that the *Legendrian connected sum* operation, denoted by $\#$, is a way of gluing Legendrian knots that preserves their orientations and tangency to the standard contact structure, creating a composite Legendrian knot. (For a formal treatment of the Legendrian connected sum operation, we refer the reader to [6].) Topologically, each crab bucket is the Legendrian connected sum of Legendrian $(2, q)$ -torus knots, as specified in Observation 1 below.

Observation 1. *The crab bucket β_5 is the Legendrian $(2, 3)$ -torus knot (i.e., the Legendrian negative trefoil). For all even $n \geq 6$, β_n is the Legendrian connected sum of Legendrian torus knots*

$$(2, 3)\#(2, 5)\#\dots\#(2, n-3)\#(2, n-3)\#(2, n-5)\#\dots\#(2, 3).$$

For all odd $n \geq 7$, the crab bucket β_n is the Legendrian connected sum of Legendrian torus knots

$$(2, 3)\#(2, 5)\#\dots\#(2, n-2)\#(2, n-4)\#\dots\#(2, 3).$$

In particular, no two crab buckets share the same smooth knot type.

Theorem 3. *Every member of the crab bucket family β_5, β_6, \dots attains the bound in Theorem 2. In particular, $m(\beta_n) = n$ for all $n \geq 5$.*

Proof. By construction, $n \geq m(\beta_n)$ for all $n \geq 5$. With this in mind, we will begin by considering all odd $n \geq 5$. By construction, every tile on the inner board of the crab bucket mosaic projection of β_n contains either a negative crossing or two cusps. Therefore, these $(n-2)^2$ inner tiles each contribute -1 to $\text{tb}(\beta_n)$. Meanwhile, the boundary tiles collectively contain $(n-1) + (n-3) = 2n-4$ cusps and no crossings, so

$$\text{tb}(\beta_n) = -(n-2)^2 - \frac{1}{2}(2n-4) = -(n-1)(n-2).$$

In particular, $\text{tb}(\beta_n) < 0$, so Theorem 2 implies that if we define

$$f(x) := \sqrt{(x-1)(x-2) - \frac{3}{4}} + \frac{3}{2},$$

then for all odd $n \geq 5$, we have

$$m(\beta_n) \geq \lceil f(n) \rceil.$$

However, $0.15 > x - f(x) > 0$ for all $x \geq 5$. (Indeed, some calculus shows that $x - f(x)$ is monotone decreasing on $(2.5, \infty)$ and converges to 0 as x tends toward infinity.) Hence, $\lceil f(n) \rceil = n$. Since $n \geq m(\beta_n)$, this proves the claim for all odd $n \geq 5$.

Now, suppose $n \geq 6$ is even. The only tiles in the inner board not containing crossings or cusps are the T_1 tile in position $(2, n-1)$ and the T_3 tile in position $(n-1, 2)$, each contributing 0 to $\text{tb}(\beta_n)$. By construction, each of the other tiles in the inner board contains either a negative crossing or two cusps. Therefore, these $(n-2)^2 - 2$ tiles each contribute -1 to $\text{tb}(\beta_n)$. Meanwhile, the boundary tiles collectively contain $(n-2) + (n-4) = 2n-6$ cusps and no crossings, so

$$\text{tb}(\beta_n) = -[(n-2)^2 - 2] - \frac{1}{2}(2n-6) = -n^2 + 3n + 1.$$

In particular, $\text{tb}(\beta_n) < 0$, so Theorem 2 implies that if we define

$$g(x) := \sqrt{x^2 - 3x - 1 - \frac{3}{4}} + \frac{3}{2},$$

then for all even $n \geq 6$, we have

$$m(\beta_n) \geq \lceil g(n) \rceil.$$

However, $0.5 > x - g(x) > 0$ for all $x \geq 6$. (Once again, some calculus shows that $x - g(x)$ is monotone decreasing on $(3.5, \infty)$ and converges to 0 as x tends toward infinity.) Hence, $\lceil g(n) \rceil = n$. Since $n \geq m(\beta_n)$, this proves the claim for all even $n \geq 6$. \square

2.3 A Linear Algebraic Approach

We now provide an alternative method for deriving bounds similar to those obtained in the previous section. Although the bounds are similar (in fact, slightly weaker), the approach is more robust.

When working with the oriented tiles in Figure 9, it is possible to track the effect each individual tile has on the classical invariants of the Legendrian knot it is a part of. For any oriented tile R_i , define $\text{tb}^*(R_i) := P - N - \frac{1}{2}C$, where P and N are the number of positive and negative crossings appearing in R_i , respectively, and C is the number of cusps appearing in R_i . In a similar fashion, define $\text{rot}^*(R_i) := \frac{1}{2}(D - U)$, where D and U are the number of downward- and upward-oriented cusps, respectively, appearing in R_i . These definitions naturally lead to the following proposition.

Proposition 2. *Let M be an oriented knot mosaic representing a Legendrian knot Λ . Then*

- i. $\text{tb}(\Lambda) = \sum_{i=0}^{24} |M|_{R_i} \text{tb}^*(R_i)$, and
- ii. $\text{rot}(\Lambda) = \sum_{i=0}^{24} |M|_{R_i} \text{rot}^*(R_i)$.

For any $0 \leq i \leq 24$, define the vector

$$\mathbf{p}_i := \begin{pmatrix} \text{tb}^*(R_i) \\ \text{rot}^*(R_i) \\ h(R_i) \\ v(R_i) \\ 1 \end{pmatrix},$$

which records relevant properties of the tile R_i . The 1 in the final coordinate will help to keep track of how many tiles are contained in the mosaic. Define the 5×25 matrix

$$P := [\mathbf{p}_0 \quad \mathbf{p}_1 \quad \dots \quad \mathbf{p}_{24}].$$

When viewed as a linear transformation from \mathbb{R}^{25} to \mathbb{R}^5 , P can be thought of as a matrix that transforms the amounts of each tile type present into a vector containing important properties describing the resulting mosaic. This idea is captured by Proposition 3.

Proposition 3. *Let M be an $n \times n$ oriented knot mosaic representing a Legendrian knot Λ . Let*

$$\mathbf{c} := \begin{pmatrix} |M|_{R_0} \\ |M|_{R_1} \\ \vdots \\ |M|_{R_{24}} \end{pmatrix}.$$

Then the product

$$P\mathbf{c} = \begin{pmatrix} \text{tb}(\Lambda) \\ \text{rot}(\Lambda) \\ 0 \\ 0 \\ n^2 \end{pmatrix}.$$

Proof. Using the definitions of P and \mathbf{c} , carrying out the matrix multiplication, and then applying Propositions 2 and 1 yields

$$P\mathbf{c} = \begin{pmatrix} \sum_{i=0}^{24} |M|_{R_i} \text{tb}^*(R_i) \\ \sum_{i=0}^{24} |M|_{R_i} \text{rot}^*(R_i) \\ \sum_{i=0}^{24} |M|_{R_i} h(R_i) \\ \sum_{i=0}^{24} |M|_{R_i} v(R_i) \\ \sum_{i=0}^{24} |M|_{R_i} \end{pmatrix} = \begin{pmatrix} \text{tb}(\Lambda) \\ \text{rot}(\Lambda) \\ 0 \\ 0 \\ n^2 \end{pmatrix}.$$

The last coordinate sums the amount of each tile type, resulting in the total number of tiles in the mosaic, n^2 . \square

We have now established the foundation needed to prove Theorem 4 below. Note that the first bound is precisely the bound in Theorem 1, and the second bound is always 1 or 2 lower than the bound in Theorem 2. While the statement of Theorem 4 does not provide any sharper restrictions on mosaic number, this alternative approach suggests that the bounds in Section 2.2 cannot be significantly improved without considering the geometric properties of Legendrian knot mosaics.

Theorem 4. *Let M be an $n \times n$ oriented Legendrian knot mosaic representing a Legendrian knot Λ .*

- i.* If $4|\text{rot}(\Lambda)| + \text{tb}(\Lambda) \geq 0$, then $m(\Lambda) \geq \left\lceil \sqrt{4|\text{rot}(\Lambda)| + \text{tb}(\Lambda)} \right\rceil$.
- ii.* If $\text{tb}(\Lambda) \leq 0$, then $m(\Lambda) \geq \left\lceil \sqrt{-\text{tb}(\Lambda)} \right\rceil$.

Proof. Consider the vector \mathbf{c} defined in Proposition 3 above. Since each $|M|_{R_i}$ is nonnegative, we have

$$\mathbf{c} \in \mathbb{R}_{\geq 0}^{25} = \{(x_1, x_2, \dots, x_{25}) \in \mathbb{R}^{25} : x_i \geq 0 \text{ for all } 1 \leq i \leq 25\}.$$

Thus, $P\mathbf{c} \in P(\mathbb{R}_{\geq 0}^{25})$, where $P(\mathbb{R}_{\geq 0}^{25})$ is the image of $\mathbb{R}_{\geq 0}^{25}$ under the linear transformation P . Define

$$V := \{(x_1, x_2, x_3, x_4, x_5) \in \mathbb{R}^5 : x_3 = x_4 = 0\}.$$

By Proposition 1, any $\mathbf{c} \in \mathbb{R}_{\geq 0}^{25}$ which represents a valid Legendrian knot mosaic will have $P\mathbf{c} \in V$. So we must have $P\mathbf{c} \in P(\mathbb{R}_{\geq 0}^{25}) \cap V$. To calculate $P(\mathbb{R}_{\geq 0}^{25})$, we

employ the right inverse of P , which we will denote as Q . (Note that Q must exist as it can be confirmed computationally that P has full rank.) Define

$$S = \{\mathbf{y} \in \mathbb{R}^5 : \text{There exists } \mathbf{v} \in \ker(P) \text{ such that } Q\mathbf{y} + \mathbf{v} \in \mathbb{R}_{\geq 0}^{25}\}.$$

We claim that $P(\mathbb{R}_{\geq 0}^{25}) = S$. If $\mathbf{y} \in S$, then for some $\mathbf{v} \in \ker(P)$,

$$\mathbf{y} = PQ\mathbf{y} + \mathbf{0} = PQ\mathbf{y} + P\mathbf{v} = P(Q\mathbf{y} + \mathbf{v}) \in P(\mathbb{R}_{\geq 0}^{25}).$$

So $S \subseteq P(\mathbb{R}_{\geq 0}^{25})$. Conversely, if $\mathbf{y} \in P(\mathbb{R}_{\geq 0}^{25})$, there exists $\mathbf{x} \in \mathbb{R}_{\geq 0}^{25}$ such that $P\mathbf{x} = \mathbf{y}$. Let $\mathbf{v} = \mathbf{x} - Q\mathbf{y}$. Then,

$$P\mathbf{v} = P(\mathbf{x} - Q\mathbf{y}) = P\mathbf{x} - PQ\mathbf{y} = \mathbf{y} - \mathbf{y} = \mathbf{0}.$$

So, $\mathbf{v} \in \ker(P)$. We also have

$$Q\mathbf{y} + \mathbf{v} = Q\mathbf{y} + \mathbf{x} - Q\mathbf{y} = \mathbf{x} \in \mathbb{R}_{\geq 0}^{25}.$$

So, by definition, $\mathbf{y} \in S$. Thus, $P(\mathbb{R}_{\geq 0}^{25}) = S$.

We can now take advantage of this fact to calculate $P(\mathbb{R}_{\geq 0}^{25})$ using the definition of S . Using a computer algebra system such as Mathematica to carry out quantifier elimination and remove all dependencies on \mathbf{v} from the system of inequalities, results in a set of inequalities which constrain $P(\mathbb{R}_{\geq 0}^{25}) \cap V$. The details of this calculation can be found in Appendix A. The calculation tells us that if $\mathbf{c} \in \mathbb{R}_{\geq 0}^{25}$, both of the following inequalities must be satisfied.

$$\begin{aligned} n^2 &\geq 4|\text{rot}(\Lambda)| + \text{tb}(\Lambda); \\ n^2 &\geq -\text{tb}(\Lambda). \end{aligned}$$

Restricting the domains to satisfy $4|\text{rot}(\Lambda)| + \text{tb}(\Lambda) \geq 0$ and $-\text{tb}(\Lambda) \geq 0$, respectively, yields

$$\begin{aligned} n &\geq \sqrt{4|\text{rot}(\Lambda)| + \text{tb}(\Lambda)}; \\ n &\geq \sqrt{-\text{tb}(\Lambda)}, \end{aligned}$$

as desired. □

3 Upper Bounds for Legendrian Unknots

3.1 Barn Tiles and Soil Setups

In [13], Pezzimenti and Pandey constructed an infinite family of Legendrian unknots called *the Kraken sequence* that realize their mosaic numbers only in non-reduced projections (i.e., projections having more than the minimum number of crossings). In this section, we define modified configurations for Legendrian n -mosaics. We also define operations on these configurations using components

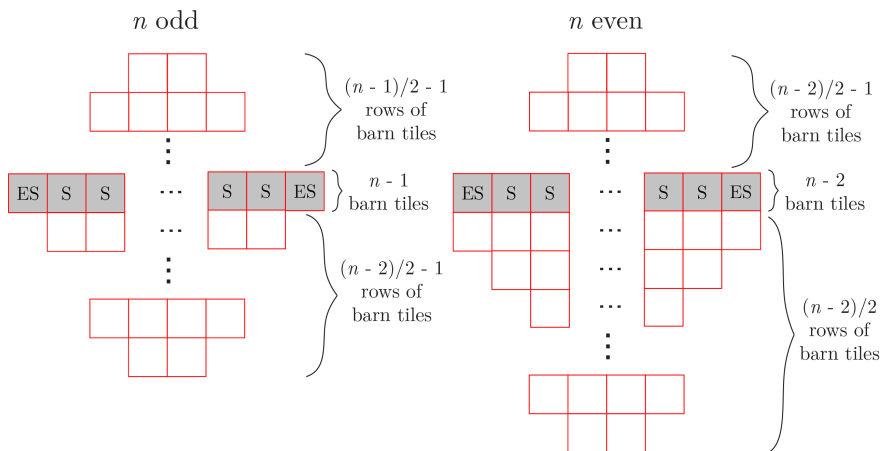


Figure 14: The default barn configuration of a Legendrian n -mosaic.

from the Kraken sequence. We will use these configurations to give a method of constructing mosaics of Legendrian unknots. From this construction, we obtain an upper bound on the mosaic number of any Legendrian unknot.

We begin the construction by defining a specified mosaic configuration. Given a Legendrian n -mosaic, a **barn configuration** is a grid formed by connecting the corners of adjacent tiles. Each resulting square is called a **barn tile**, named so because the “X”-shape in each barn tile resembles the cross-brace design on sliding barn doors. Explicit examples of barn tiles are shown in Figures 15 and 16.

While there are several valid barn configurations of a particular n -mosaic, we are interested in the one such that the tile in position $(1, n)$ is not contained in any barn tiles. We call this specific barn configuration the **default barn configuration**. In the default barn configuration, there are $n - 2$ rows of barn tiles. In particular, if n is odd, there are rows of barn tiles of lengths $2, 4, \dots, n - 1, n - 3, \dots, 2$, going from top to bottom. If n is even, there are rows of barn tiles of lengths $2, 4, \dots, n - 2, n - 2, n - 4, n - 6, \dots, 2$, going from top to bottom. Figures 14 and 15 depict the geometry of the default barn configuration for both odd and even n .

We begin to fill the default barn configuration with tiles as follows. Let $i := 0$ if n is odd and $i := 1$ if n is even. Let the mosaic tiles in positions $(1, 1 + i)$ and $(n - i, n)$ be T_2 and T_4 , respectively. Also, let the tiles in positions $(1, 2 + i), (2, 3 + i), \dots, (n - 1 - i, n)$ be T_1 . Likewise, let the tiles in positions $(2, 1 + i), (3, 2 + i), \dots, (n - i, n - 1)$ be T_3 . Now, consider the $n - 2 - i$ mosaic tiles in positions $(2, 2 + i), (3, 3 + i), \dots, (n - 1 - i, n - 1)$, and let each of them be either T_7 or T_{10} . We call the $n - 1 - i$ barn tiles intersecting these mosaic tiles **soil tiles**. In particular, we call the leftmost and rightmost soil tiles **edge-soil tiles**. Note that the soil tiles are precisely the barn tiles in the $[(n - 1 - i)/2]$ th row of barn tiles.

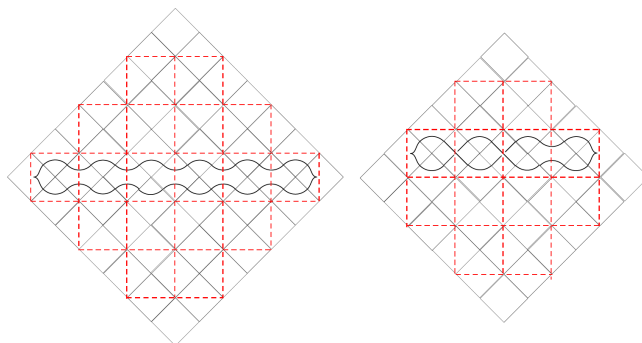


Figure 15: A Legendrian 7-mosaic and a Legendrian 6-mosaic, each having a soil setup. Note that each mosaic depicts an unknot.

If we insert tiles in a Legendrian n -mosaic having the default barn configuration exactly as described above, then we say the resulting mosaic has a **soil setup**. Figure 15 gives examples of soil setups for $n = 7$ and $n = 6$. Note that any barn tile in a soil setup is empty if and only if it is not a soil tile. By construction, we have the following:

Observation 2. *If M is a Legendrian n -mosaic having a soil setup, then M depicts a Legendrian unknot Λ_U with $\text{tb}(\Lambda_U) = -|M|_{T_{10}} - 1$. Moreover, $\text{rot}(\Lambda_U) = 0$ if $|M|_{T_{10}}$ is even, and $\text{rot}(\Lambda_U) = \pm 1$ if $|M|_{T_{10}}$ is odd.*

The last part of this observation follows from the fact that the two cusps in the edge-soil tiles of M share the same orientation if and only if $|M|_{T_{10}}$ is odd.

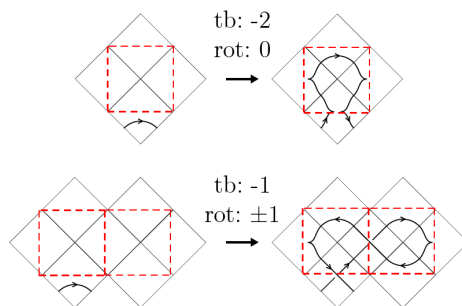


Figure 16: The Kraken (top) and fish (bottom) moves and their effects on the classical invariants.

Next, we define two moves which will “fill” the non-soil barn tiles. The resulting structures will appear to “grow out of the soil” vertically. The first of these moves is inspired by the Kraken sequence of [13]. Consider an empty barn tile inscribed in four mosaic tiles. Among these four mosaic tiles, suppose that either the bottom tile is T_1 or the top tile is T_3 . Then, we define the **Kraken**

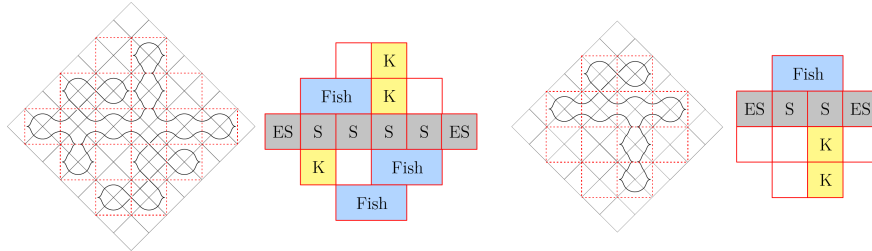


Figure 17: Two Legendrian n -mosaics, each created by performing Kraken and fish moves on a mosaic having a soil setup. Note that these mosaics depict stabilized Legendrian unknots.

move as the move depicted in the first row of Figure 16, up to reflection about the horizontal axis.

Now, consider two adjacent empty barn tiles inscribed in seven mosaic tiles. Among these seven mosaic tiles, suppose that at least one of the following is true: one or both of the bottommost tiles is T_1 , or one or both of the topmost tiles is T_3 . Then, we define the **fish move** (named for its fish-like appearance) as the move depicted in the second row of Figure 16, up to reflections about the horizontal axis, the vertical axis, or both axes. Note that the fish move changes one of the aforementioned T_1 or T_3 tiles to a T_{10} tile.

By Figure 16, performing a fish move on two empty barn tiles changes both of the mosaic tiles containing the top (resp. bottom) edges of those barn tiles to T_1 (resp. T_3). A similar statement holds for Kraken moves. In a soil setup, the mosaic tile containing the top (resp. bottom) edge of any soil tile is also T_1 (resp. T_3). Therefore, we have the following:

Observation 3. *If M is a Legendrian n -mosaic with a soil setup and M' is obtained by performing any number of fish and Kraken moves on M , then we can perform a Kraken move on any empty barn tile in M' that lies directly above or beneath a nonempty barn tile. Similarly, we can perform a fish move on any pair of adjacent empty tiles in M' that lie directly above or beneath a nonempty barn tile.*

In other words, we can “stack” fish and Kraken moves on vertically adjacent barn tiles. Figures 17, 18, and 19 give examples of Legendrian n -mosaics produced by performing fish and Kraken moves on a soil setup in this fashion.

This observation also implies a necessary and sufficient condition for f fish moves and k Kraken moves to be possible on a mosaic having a soil setup:

Lemma 2. *Let M be a Legendrian n -mosaic having a soil setup. Then it is possible to perform f fish moves and k Kraken moves on M if and only if*

$$2f + k \leq N,$$

where

$$N := \begin{cases} \frac{(n-1)(n-3)}{2}, & 2 \nmid n \\ \frac{(n-2)^2}{2}, & 2 \mid n. \end{cases}$$

Proof. Since M has a soil setup, N is the number of non-soil barn tiles (equivalently, the number of empty barn tiles) appearing in M . Since fish moves fill two adjacent empty barn tiles and Kraken moves fill one empty barn tile, the necessity of the condition $2f + k \leq N$ is clear.

Sufficiency follows from Observation 3 and the fact that every row of barn tiles in M contains an even number of barn tiles. Note that if we label the barn tiles in each row of barn tiles as B_1, \dots, B_m going left to right, then we perform fish moves only on pairs B_i, B_{i+1} where i is odd. \square

Moreover, the Kraken move introduces two upward-oriented cusps and two downward-oriented cusps, while the fish move introduces two cusps of the same orientation, one positive trivial crossing, and one negative trivial crossing. Figure 16 shows the effects of Kraken and fish moves on the Thurston-Bennequin number and rotation number. Furthermore, we have the following:

Lemma 3. *Let M be a Legendrian n -mosaic having a soil setup. Let M' be a mosaic obtained by performing k Kraken moves and f fish moves on M . Then M' depicts a Legendrian unknot Λ_U whose Thurston-Bennequin number is*

$$\text{tb}(\Lambda_U) = -2k - f - |M|_{T_{10}} - 1.$$

Moreover, if $|M|_{T_{10}}$ is odd, then

$$|\text{rot}(\Lambda_U)| = f + 1.$$

Proof. All crossings introduced by Kraken and fish moves are trivial, and neither move introduces any “loose strands.” It follows from Observation 2 that M' depicts a Legendrian unknot Λ_U . Combining Observation 2 with Figure 16 yields the desired Thurston-Bennequin number. Now, if $|M|_{T_{10}}$ is odd, then all cusps introduced by fish moves share the same orientation as the two cusps in the edge-soil tiles of M' . Therefore, combining Observation 2 with Figure 16 gives us the desired expression for $|\text{rot}(\Lambda_U)|$. \square

3.2 Results

In the proof of the bound in Theorem 5 and Corollary 1 below, we present an algorithm to construct a mosaic for any Legendrian unknot. The algorithm begins with a specified soil setup. Then, it performs specified numbers of Kraken and fish moves to achieve the desired classical invariants.

Note that the expressions under the radicals in (5) and (8) are always positive since $\text{tb}(\Lambda_U) \leq -2$ for any Legendrian unknot Λ_U satisfying $\text{rot}(\Lambda_U) \neq 0$. Similarly, the expression under the radical in (6) is always positive since the maximum Thurston-Bennequin number across all Legendrian unknots is -1 .

Theorem 5. *Let Λ_U be a Legendrian unknot. If $\text{rot}(\Lambda_U) \neq 0$, then*

$$m(\Lambda_U) \leq \left\lceil \sqrt{3|\text{rot}(\Lambda_U)| - \text{tb}(\Lambda_U) - \frac{11}{4}} + \frac{3}{2} \right\rceil. \quad (5)$$

If $\text{rot}(\Lambda_U) = 0$, then

$$m(\Lambda_U) \leq \left\lceil \sqrt{-\text{tb}(\Lambda_U) + \frac{5}{4}} + \frac{3}{2} \right\rceil. \quad (6)$$

Proof. Let $r := |\text{rot}(\Lambda_U)|$. For $r \neq 0$, we will construct a Legendrian n -mosaic for Λ_U with

$$n := \left\lceil \sqrt{3r - \text{tb}(\Lambda_U) - \frac{11}{4}} + \frac{3}{2} \right\rceil.$$

To that end, let M be the unique Legendrian n -mosaic having a soil setup with no T_7 tiles. In other words, all non-edge soil tiles of M contain crossings, so

$$|M|_{T_{10}} = \begin{cases} n-2, & 2 \nmid n \\ n-3, & 2 \mid n. \end{cases}$$

In particular, $|M|_{T_{10}}$ is odd.

Now, set $f := r - 1$, and set

$$k := \begin{cases} -\frac{1}{2}(\text{tb}(\Lambda_U) + r + n - 2), & 2 \nmid n \\ -\frac{1}{2}(\text{tb}(\Lambda_U) + r + n - 3), & 2 \mid n. \end{cases} \quad (7)$$

Note that since $\text{tb}(\Lambda_U)$ and r have different parities, $\text{tb}(\Lambda_U) + r$ is odd. Thus, in either case, $k \in \mathbb{Z}$. Furthermore,

$$\text{tb}(\Lambda_U) = \begin{cases} -2k - r - n + 2, & 2 \nmid n \\ -2k - r - n + 3, & 2 \mid n. \end{cases}$$

Now, note that the inequality $n \geq \sqrt{3r - \text{tb}(\Lambda_U) - 11/4} + 3/2$ implies the inequality

$$n^2 - 3n + \frac{9}{4} \geq 3r - \text{tb}(\Lambda_U) - \frac{11}{4}.$$

If n is odd, algebraically manipulating this inequality yields

$$\frac{(n-1)(n-3)}{2} \geq 2(r-1) - \frac{1}{2}(\text{tb}(\Lambda_U) + r + n - 2) = 2f + k.$$

If instead n is even, algebraic manipulation yields

$$\frac{(n-2)^2}{2} \geq 2(r-1) - \frac{1}{2}(\text{tb}(\Lambda_U) + r + n - 3) = 2f + k.$$

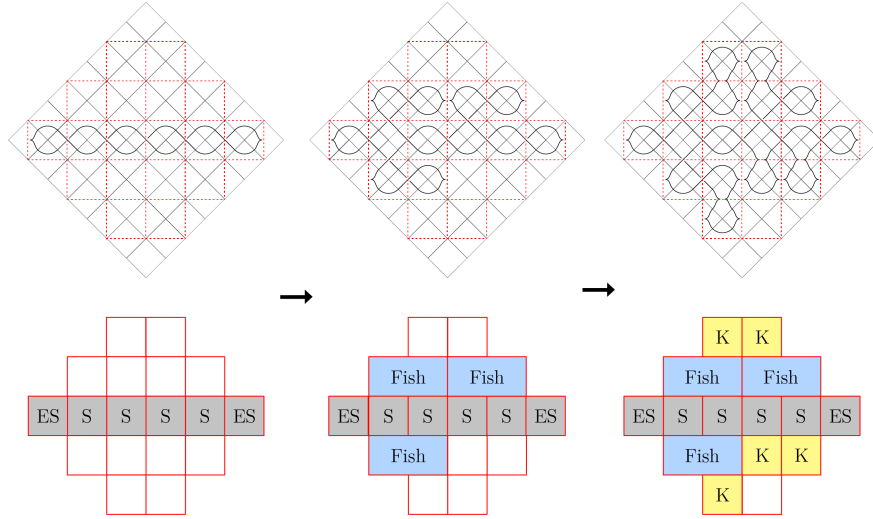


Figure 18: Using the algorithm from the proof of Theorem 5 to construct a mosaic for the Legendrian unknot Λ_U with $\text{tb}(\Lambda_U) = -19$ and $\text{rot}(\Lambda_U) = 4$.

It follows from Lemma 2 that we can perform k Kraken moves and f fish moves on M . By Lemma 3, the resulting mosaic depicts a stabilized Legendrian unknot $\Lambda_{U'}$. Figure 18 gives an example of such a construction.

We claim that $\Lambda_{U'}$ and Λ_U are Legendrian isotopic. To show this, it will be enough to show that these unknots share the same Thurston-Bennequin invariant and rotation number (cf. [3]). To that end, note by Lemma 3 that

$$|\text{rot}(\Lambda_{U'})| = f + 1 = r = |\text{rot}(\Lambda_U)|,$$

as desired. (This equality is sufficient since if $\text{rot}(\Lambda_{U'}) = -\text{rot}(\Lambda_U)$, then we can simply choose the opposite orientation of $\Lambda_{U'}$ to invert the sign of $\text{rot}(\Lambda_{U'})$.) Lemma 3 also implies that if n is odd, then

$$\begin{aligned} \text{tb}(\Lambda_{U'}) - 2k - f - (n - 2) - 1 &= -2k - (r - 1) - (n - 2) - 1 \\ &= -2k - r - n + 2 \\ &= \text{tb}(\Lambda_U), \end{aligned}$$

as desired. If n is even, a similar calculation shows that

$$\text{tb}(\Lambda_{U'}) = -2k - r - n + 3 = \text{tb}(\Lambda_U),$$

so in either case, $\Lambda_{U'}$ and Λ_U are Legendrian isotopic.

If instead $r = 0$, let

$$n := \left\lceil \sqrt{-\text{tb}(\Lambda_U) + \frac{5}{4} + \frac{3}{2}} \right\rceil,$$

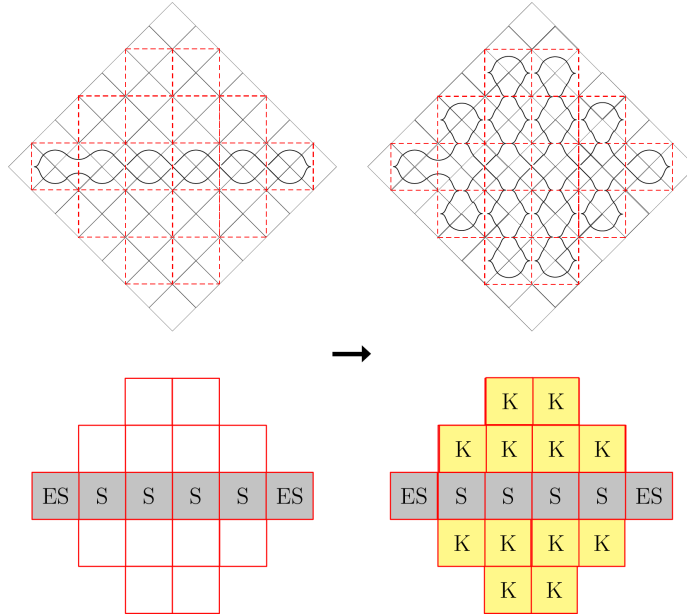


Figure 19: Using the algorithm from the proof of Theorem 5 to construct a mosaic for the Legendrian unknot Λ_U with $\text{tb}(\Lambda_U) = -29$ and $\text{rot}(\Lambda_U) = 0$.

and use this value of n to define k exactly as we did in (7). This time, let M be a Legendrian n -mosaic having a soil setup with exactly one T_7 tile, so that

$$|M|_{T_{10}} = \begin{cases} n-3, & 2 \nmid n \\ n-4, & 2 \mid n. \end{cases}$$

In particular, $|M|_{T_{10}}$ is even. It follows from Observation 2 that the Legendrian unknot depicted in M has rotation number 0.

Similarly to before, note that the inequality $n \geq \sqrt{-\text{tb}(\Lambda_U) + 5/4} + 3/2$ implies the inequality

$$n^2 - 3n + \frac{9}{4} \geq -\text{tb}(\Lambda_U) + \frac{5}{4}.$$

If n is odd, algebraically manipulating this inequality yields

$$\frac{(n-1)(n-3)}{2} \geq -\frac{1}{2}(\text{tb}(\Lambda_U) + n - 2) = k.$$

If instead n is even, algebraic manipulation yields

$$\frac{(n-2)^2}{2} \geq -\frac{1}{2}(\text{tb}(\Lambda_U) + n - 3) = k.$$

It follows from Lemma 2 that we can perform k Kraken moves on M . (We will not perform any fish moves on M .) The resulting mosaic depicts a Legendrian unknot $\Lambda_{U'}$. Figure 19 gives an example of such a construction.

Once again, it will be enough to show that the classical invariants of $\Lambda_{U'}$ equal those of Λ_U . By Figure 16, the fact that we did not perform any fish moves on M implies that

$$\text{rot}(\Lambda'_{U'}) = 0 = \text{rot}(\Lambda_U),$$

as desired. To compute the Thurston-Bennequin number, we once again appeal to Lemma 3. If n is odd, then

$$\text{tb}(\Lambda_{U'}) = -2k - (n - 3) - 1 = -2k - r - n + 2 = \text{tb}(\Lambda_U),$$

as desired. If n is even, then a similar calculation yields

$$\text{tb}(\Lambda_{U'}) = -2k - r - n + 3 = \text{tb}(\Lambda_U),$$

so in either case, $\Lambda'_{U'}$ is Legendrian isotopic to Λ_U . This completes the proof. \square

In particular, we have the following for Legendrian unknots on the “outermost boundary” of their mountain range:

Corollary 1. *Let Λ_U be a Legendrian unknot with $\text{rot}(\Lambda_U) \neq 0$, and suppose $\text{tb}(\Lambda_U) = -|\text{rot}(\Lambda_U)| - 1$ (i.e., $\text{rot}(\Lambda_U)$ is either minimal or maximal among the rotation numbers of all other Legendrian unknots sharing the same Thurston-Bennequin invariant as Λ_U). Then*

$$m(\Lambda_U) \leq \left\lceil \sqrt{-4 \text{tb}(\Lambda_U) - \frac{23}{4} + \frac{3}{2}} \right\rceil = \left\lceil \sqrt{4|\text{rot}(\Lambda_U)| - \frac{7}{4} + \frac{3}{2}} \right\rceil. \quad (8)$$

4 The Number of Legendrian Link Mosaics

In Theorem 1 of [12], Oh, Hong, Lee, and Lee give an algorithm to count the number, which they call $D^{(m,n)}$, of $m \times n$ classical link mosaics. In this section, we adapt their result to the Legendrian setting. Let $\mathbb{L}^{(m,n)}$ denote the set of $m \times n$ Legendrian link mosaics (i.e., suitably connected mosaics using only the mosaic tiles in Figure 7), and let $D_L^{(m,n)}$ denote the total number of elements in $\mathbb{L}^{(m,n)}$. We will prove the following algorithm to compute $D_L^{(m,n)}$ for any $m, n \in \mathbb{Z}^+$. Here, $\|M\|$ denotes the sum of all entries of a matrix M .

Theorem 6. *Let $m, n \in \mathbb{Z}^+$. If $m = 1$ or $n = 1$, then the total number $D_L^{(m,n)}$ of all $m \times n$ Legendrian link mosaics is 1. Otherwise,*

$$D_L^{(m,n)} = 2\|(X_{m-2} + O_{m-2})^{n-2}\|,$$

where X_{m-2} and O_{m-2} are $2^{m-2} \times 2^{m-2}$ matrices defined recursively by

$$X_{k+1} := \begin{bmatrix} X_k & O_k \\ O_k & X_k \end{bmatrix} \quad \text{and} \quad O_{k+1} := \begin{bmatrix} O_k & X_k \\ X_k & 3O_k \end{bmatrix}$$

for $k = 0, 1, \dots, m-3$, with 1×1 matrices $X_0, O_0 := [1]$. For $n = 2$, by $(X_{m-2} + O_{m-2})^0$ we mean the $2^{m-2} \times 2^{m-2}$ identity matrix.

Proof. If $m = 1$ or $n = 1$, then $D_L^{(m,n)} = 1$ since the only way for a single row or column of Legendrian mosaic tiles to be suitably connected is for all of its tiles to be T_0 . So, suppose $m, n \geq 2$. Let $\mathbb{K}_{T_9}^{(m,n)}$ be the set of $m \times n$ classical link mosaics that do not contain any T_9 tiles, and let $D_{T_9}^{(m,n)}$ be the total number of elements of $\mathbb{K}_{T_9}^{(m,n)}$. We claim that $D_L^{(m,n)} = D_{T_9}^{(m,n)}$. Indeed, by the construction of the Legendrian mosaic tiles in [13], rotating counterclockwise by 45° and replacing vertical tangencies with cusps gives a bijection from $\mathbb{K}_{T_9}^{(m,n)}$ to $\mathbb{L}^{(m,n)}$.

So, it suffices to compute $D_{T_9}^{(m,n)}$. We first refer the reader to the proof of Theorem 1 in [12] that computes $D^{(m,n)}$. In that proof, the authors assign *states* to each suitably connected classical $m \times n$ mosaic that record the number and locations of connection points on the edges of each mosaic tile. Their algorithm for computing $D^{(m,n)}$ relies on recurrence relations of *state matrices*, which are block matrices whose entries count the number of suitably connected mosaics of a certain size and with a given state. Due to this proof's length and complexity, we will not reproduce every detail here.

Instead, we adjust the proof slightly by removing T_9 from the set of allowable tiles. In particular, T_7 , T_8 , and T_{10} are the only usable tiles with at least three connection points. Therefore, the “four” in the statement of the *choice rule* stated in Section 2 of [12] changes to “three.” Similarly, these three tiles are now the only tiles counted by the $(2, 2)$ -entry of the state matrix O_1 defined in this section. Thus, the state matrices defined in this section are now

$$X_1 = \begin{bmatrix} 1 & 1 \\ 1 & 1 \end{bmatrix}, \quad O_1 = \begin{bmatrix} 1 & 1 \\ 1 & 3 \end{bmatrix}, \quad \text{and} \quad N^{(1,1)} = X_1 + O_1 = \begin{bmatrix} 2 & 2 \\ 2 & 4 \end{bmatrix}.$$

In particular, the bottom-right submatrix of O_{k+1} in the inductive step of Proposition 2 in [12] becomes $3O_k$ rather than $4O_k$. Since these are the only points in the proof where T_9 tiles have any bearing, the rest of the proof in [12] shows that $D_{T_9}^{(m,n)}$ is given by the formula in the statement of Theorem 6. \square

In particular, $D_L^{(m,2)} = D^{(m,2)}$ for all $m \in \mathbb{Z}^+$ since T_9 tiles do not appear in classical link mosaics with only two rows or columns. As noted in [12], this quantity is precisely 2^{m-1} .

By implementing the algorithm of Theorem 6 in Mathematica, we were able to compute $D_L^{(m,n)}$ for all $1 \leq n \leq m \leq 11$. We present our code and data in Appendix B.

In [12], the authors computed $D^{(n,n)}$ for all $n \leq 13$. This allows us to consider the ratios

$$\delta(n) := \frac{D_L^{(n,n)}}{D^{(n,n)}}$$

for all $n \leq 11$. Similarly to $D^{(n,n)}$, it appears that $D_L^{(n,n)}$ grows at a quadratic exponential rate. Moreover, $\delta(n)$ seems to monotonically converge to 0 at a quadratic exponential rate. We provide graphs and best-fit models of $\ln D_L^{(n,n)}$ and $\ln \delta(n)$ in Figures 20 and 21, respectively.

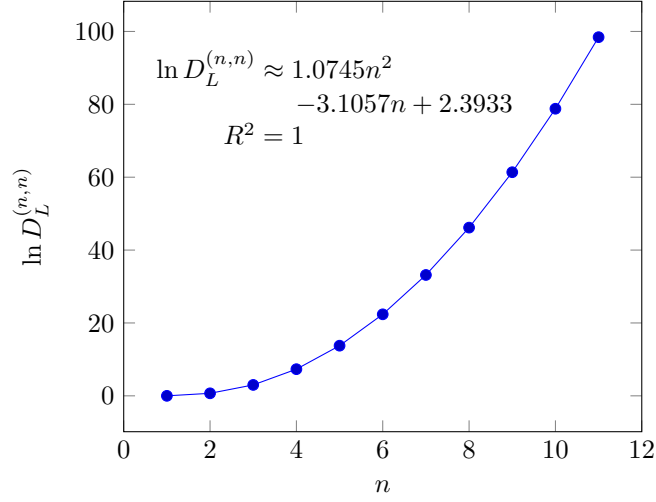


Figure 20: Quadratic exponential growth of the number $D_L^{(n,n)}$ of suitably connected Legendrian n -mosaics.

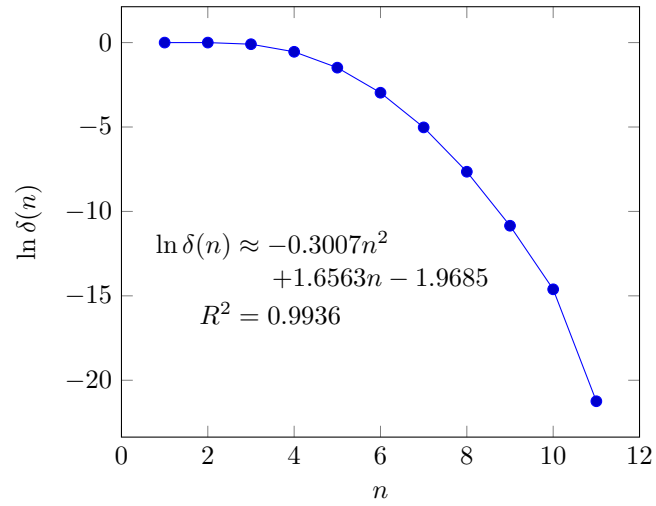


Figure 21: Negative quadratic exponential growth of the ratios $\delta(n)$ between the number $D_L^{(n,n)}$ of suitably connected Legendrian n -mosaics and the number $D^{(n,n)}$ of suitably connected classical n -mosaics.

5 Updated Censuses

In [13], Pezzimenti and Pandey give a preliminary census containing computed mosaic numbers of certain Legendrian knots, organized in their mountain ranges, as introduced in Section 1.1. Using an exhaustive computer search, we provide an updated census, which covers a much larger class of Legendrian knots. The updated mountain ranges are give in Appendix C.

While the exact mosaic number of a Legendrian knot is generally hard to determine, precise bounds can be obtained via an exhaustive search. Suppose L_n is the set containing every Legendrian knot realizable on a Legendrian n -mosaic. If $\Lambda \in L_n$, then $m(\Lambda) \leq n$, and, likewise, if $\Lambda \notin L_n$, then $m(\Lambda) > n$. These lists would be impractical to produce by hand, but the discrete nature of this problem makes it a natural fit for a computer search. In this section, we detail such a computer search and summarize its results, using the mountain ranges provided in [1] as a base for our censuses.

5.1 Computer Search

Our search was conducted using two programs: `mosaic-gen.rs`, a `rust` program that produces a list of all suitably connected Legendrian n -mosaics for a given n , and `mosaic-cat.py`, a `python` program that catalogs those mosaics by `tb`, `rot`, and smooth knot type. Full implementations and documentation for these programs can be found in [10].

When working digitally, it is convenient to represent mosaics as integers in base-10, obtained by reading a mosaic's tile numbers from left to right and top to bottom, starting from the left corner as shown in in Figure 22. Here, we use 9 instead of 10 to represent the crossing tile T_{10} for ease of notation, as T_9 is unused in Legendrian mosaics.

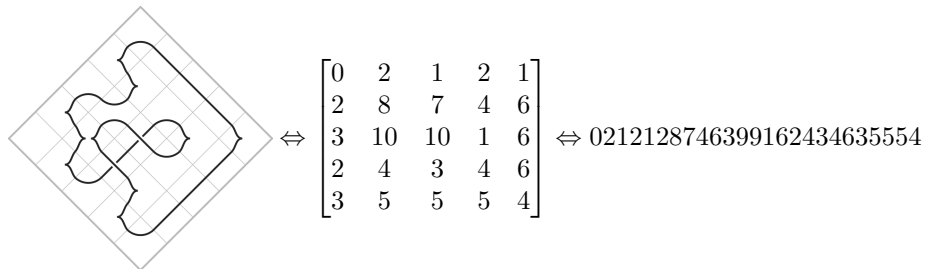


Figure 22: Representing a Legendrian mosaic as an integer.

Using this representation, a list of all suitably connected n -mosaics can be obtained by simply iterating through all positive integers in base-10 of maximum length n^2 , and noting those mosaics that are suitably connected. This process

Mosaic Size	Maximum tb	Minimum tb	Maximum rot
$n = 2$	-1	-1	0
$n = 3$	-1	-3	2
$n = 4$	-1	-7	2
$n = 5$	1	-12	3
$n = 6$	3	-21	6

Table 1: Computationally verified bounds on tb and rot.

Mosaic Size	Realizable Smooth Knots
$n = 2$	0_1
$n = 3$	0_1
$n = 4$	0_1
$n = 5$	$0_1, 3_1, m(3_1)$
$n = 6$	$0_1, 3_1, m(3_1), 3_1\#3_1, m(3_1)\#m(3_1), 4_1, 5_1, m(5_1), 5_2, m(5_2), 6_1, m(6_1), 7_1, m(7_1), 7_2, m(7_2), 8_1, m(8_1)$

Table 2: Smooth knot types realizable on a Legendrian n -mosaic.

is handled by `mosiac-gen.rs`, which produces lists matching the numbers of Legendrian link mosaics presented in Section 4 and Appendix B.

From this list, `mosaic-cat.py` determines which mosaics correspond to knots (rather than links). If so, the classical invariants of the associated knot are noted, and the knot is encoded as an extended Gauss code to be used with SageMath’s `Links` package [16]. This package is used to calculate the HOMFLY-PT polynomial of the resulting knots, which, for knots up to 8 crossings, uniquely determines the smooth knot type [14]. This was a valid assumption for the mosaic sizes that we cataloged. Our mosaics are then organized into a list according to their smooth knot type, Thurston-Bennequin number, and rotation number.

5.2 Results

Using the programs described in Section 5.1, we produced lists of all Legendrian knots, distinct up to smooth knot type and classical invariants, realizable on mosaics through size 6. The results from these lists regarding the knots (both smooth and Legendrian) realizable on a given mosaic size are summarized in Tables 1, 2, and 3.

The bounds from these lists were also used to create updated censuses for every smooth knot type found, with one caveat. While the lower bound indicated in a census applies to every Legendrian representative with the given tb and rot, upper bounds only indicate that at least one Legendrian representative with those classical invariants is realizable on a mosaic of that size. For certain smooth knot types, for instance 5_1 , multiple non-isotopic Legendrian representatives may have the same classical invariants, but the upper bound may not

Mosaic Size	Mosaics corresponding to knots	Distinct Legendrian knots
$n = 2$	1	1
$n = 3$	17	4
$n = 4$	793	9
$n = 5$	275557	40
$n = 6$	831699599	328

Table 3: Number of distinct suitably connected square Legendrian n -mosaics corresponding to knots (rather than links), and number of distinct Legendrian knots within these mosaics.

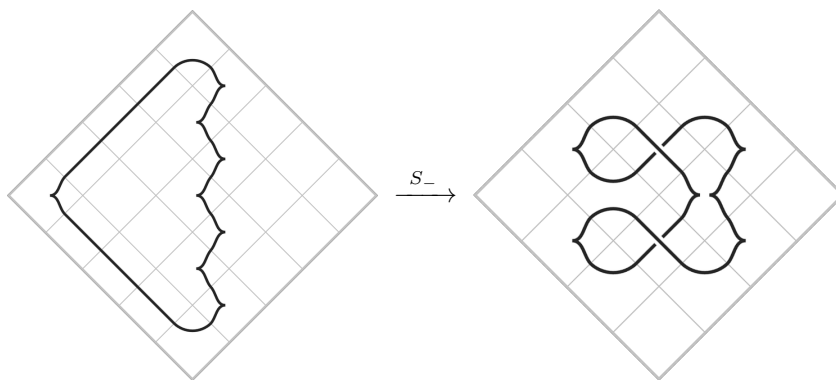


Figure 23: Stabilization reducing mosaic number in the unknot.

apply to every representation. More information on these smooth knot types can be found in [1].

The full updated censuses are available in Appendix C, and minimal mosaics for the knots presented in these censuses can be found in Appendix D.

The lower bounds provided by this search answered many of the questions presented by Pezzimenti and Pandey in [13] and reintroduced in Section 1.3, particularly those regarding how stabilization affects mosaic number:

Observation 4. *There exist (several) Legendrian knots for which stabilization reduces mosaic number.*

Examples of occurrences of Legendrian knots featuring this property are highlighted in yellow in the mountain ranges of Appendix C. One of the simplest examples of a mosaic-number-reducing stabilization, and the only example of a knot with mosaic number 5 being stabilized to a knot with mosaic number 4, can be found in the census for the unknot (Figure C.1) and is depicted in Figure 23.

The crab buckets introduced in Section 2.2 are inspired by an unusual example from the negative trefoil census (Figure C.2). While most stabilizations

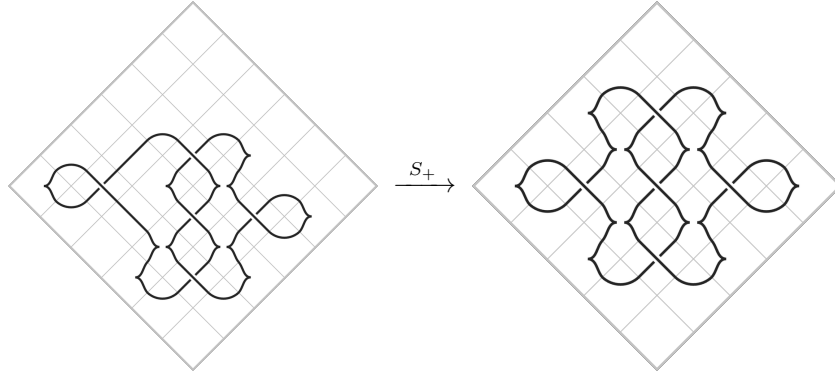


Figure 24: Stabilization producing β_5 .

reduce the magnitude of the a knot’s rotation number and occur towards the edges of the census, the crab bucket β_5 is the result of a stabilization that increases the magnitude of the rotation number, depicted in Figure 24. In Figure C.2, β_5 is the knot with $\text{tb}(\beta_5) = -12$ and $\text{rot}(\beta_5) = 1$, near the middle of the census.

Observation 5. *There exists a smooth knot K for which $m_L(K)$ is only realized by a Legendrian representative with non-maximal Thurston-Bennequin number, namely 8_1 .*

In other words, there exists a smooth knot whose Legendrian mosaic number is not obtained by a “peak” on its mountain range. In fact, the Legendrian knot at the peak of the mountain range for 8_1 requires two stabilizations, one positive and one negative, to realize Legendrian mosaic number of 8_1 , as shown in Figure 25. Our search concluded that $m_L(8_1) = 6$, while $m(\Lambda) = 7$, where Λ is the Legendrian representative of 8_1 with maximal Thurston-Bennequin invariant.

This can also be seen in the censuses for 5_1 and 7_1 (Figures C.5 and C.8), both of which contain multiple peaks in their mountain ranges. Both knots have at least one Legendrian representative of with maximal Thurston-Bennequin invariant that does not realize its Legendrian mosaic number (although, other peaks do).

6 Further Questions

We conclude by suggesting some additional related areas to explore. Since our computer search showed that the Legendrian mosaic number of 8_1 is not attained by any Legendrian representative with maximal Thurston-Bennequin invariant, it is natural to ask whether infinitely many such knot types exist:

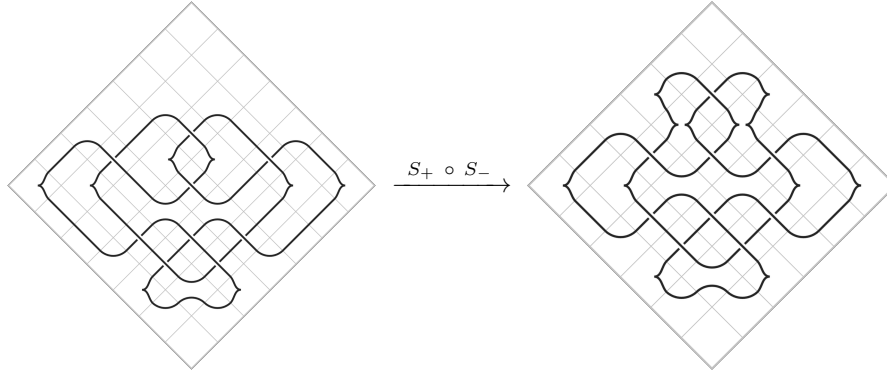


Figure 25: Maximum tb and minimum mosaic number representations of 8_1 .

Question 1. *Are there infinitely many smooth knot types whose Legendrian mosaic number is only attained by stabilized Legendrian representatives?*

Similarly, our computer search produced examples of stabilization decreasing the mosaic number. This leads us to ask the (weaker) question of whether infinitely many such examples exist:

Question 2. *Are there infinitely many Legendrian knots for which stabilization decreases the mosaic number?*

Our original motivation behind the crab bucket construction at the end of Section 2.2 was to answer this question by providing an infinite family of Legendrian knots for which stabilization decreases the mosaic number. The name of our construction alludes to the so-called “crabs in a bucket effect.” For all odd $n \geq 5$, any attempt to stabilize a cusp of β_n seems to be prevented by its neighboring cusps and crossings, like crabs in a bucket pulling each other back in whenever one attempts to escape:

Conjecture 1. *For all odd $n \geq 5$, fix an orientation of the crab bucket β_n so that $\text{rot}(\beta_n) = 1$. Then β_n cannot be negatively destabilized without increasing its mosaic number.*

As discussed in Section 5, this holds when $n = 5$. Since the crossing number and classification of connected sums of Legendrian torus knots are well-understood (see, for example, [2] or [6]), answering the following question may aid in proving our conjecture:

Question 3. *Can we improve upon the bounds in Section 2 by considering the crossing number or other invariants of Legendrian knots?*

Of course, this question is intriguing in its own right. In particular, it would be interesting to incorporate the crossing number into the linear algebraic approach discussed in Section 2.3.

Furthermore, our upper bound construction in Section 3 is limited only to Legendrian unknots. It would be desirable to generalize the resulting bounds to Legendrian representatives of other smooth knot types:

Question 4. *Can we obtain upper bounds for the mosaic number of Legendrian nontrivial knots, by reworking the barn tile construction or otherwise?*

One way to rework the soil setup construction for a given Legendrian nontrivial knot Λ might be to fix some pre-stabilized copy Λ' of Λ in the corner of a mosaic and place soil tiles adjacent to Λ' before performing Kraken and fish moves. Another way might be to consider moves other than Kraken and fish moves on barn tiles.

However, this construction may become less optimal as the rotation number increases. Namely, the only way to increase the rotation number in our construction is to use fish moves, each of which fills two barn tiles. As a consequence, Theorem 5 places the four Legendrian unknots with rotation number 6 and Thurston-Bennequin invariants $-7, -9, -11,$ and -13 on a Legendrian 7-mosaic, while our computer search produced a Legendrian 6-mosaic for these unknots. This motivates the following question:

Question 5. *Can our bound in Theorem 5 be improved using a different construction?*

In particular, it would be desirable to decrease the coefficient on the term $3|\text{rot}(\Lambda_U)|$ in our current bound. One approach could be to consider moves other than fish moves that affect the rotation number.

Finally, it is reasonable to alter the computer algorithm from Section 5 to generate random Legendrian knot and link mosaics. The following question, then, extends the growing literature on random knots (see, for example, [9] or [8]) to the study of Legendrian knots and knot mosaics:

Question 6. *What can random Legendrian knot mosaic generation tell us about the distributions of Legendrian knots and their invariants across all Legendrian knot mosaics of a given size?*

Acknowledgments

We would like to thank Eugene Fiorini for encouraging us to publish some of our findings on the Online Encyclopedia of Integer Sequences. We would also like to thank the developers of the computer game *Minecraft*, in which using a custom resource pack greatly facilitated our conception of the constructions in Section 3.

This research was done at Moravian University as part of the Research Challenges of Computational Methods in Discrete Mathematics REU; it was funded by the National Science Foundation (MPS-2150299).

References

- [1] Wutichai Chongchitmate and Lenhard Ng, *An atlas of Legendrian knots*, Exp. Math. **22** (2013), no. 1, 26–37. MR3038780
- [2] Yuanan Diao, *The additivity of crossing numbers*, J. Knot Theory Ramifications **13** (2004), no. 7, 857–866. MR2101230
- [3] Yakov Eliashberg and Maia Fraser, *Topologically trivial Legendrian knots*, J. Symplectic Geom. **7** (2009), no. 2, 77–127. MR2496415
- [4] John B. Etnyre, *Legendrian and transversal knots*, Handbook of knot theory, 2005, pp. 105–185. MR2179261
- [5] John B. Etnyre and Ko Honda, *Knots and contact geometry. I. Torus knots and the figure eight knot*, J. Symplectic Geom. **1** (2001), no. 1, 63–120. MR1959579
- [6] ———, *On connected sums and Legendrian knots*, Adv. Math. **179** (2003), no. 1, 59–74. MR2004728
- [7] John B. Etnyre, Lenhard L. Ng, and Vera Vértési, *Legendrian and transverse twist knots*, J. Eur. Math. Soc. (JEMS) **15** (2013), no. 3, 969–995. MR3085098
- [8] Chaim Even-Zohar, *Models of random knots*, J. Appl. Comput. Topol. **1** (2017), no. 2, 263–296. MR3975555
- [9] Chaim Even-Zohar, Joel Hass, Nati Linial, and Tahl Nowik, *Invariants of random knots and links*, Discrete Comput. Geom. **56** (2016), no. 2, 274–314. MR3530968
- [10] Margaret Kipe, *Legendrian-Knot-Mosaics*, 2024. <https://github.com/margekk/Legendrian-Knot-Mosaics>.
- [11] Samuel J. Lomonaco and Louis H. Kauffman, *Quantum knots and mosaics*, Quantum Inf. Process. **7** (2008), no. 2-3, 85–115. MR2420814
- [12] Seungsang Oh, Kyungpyo Hong, Ho Lee, and Hwa Jeong Lee, *Quantum knots and the number of knot mosaics*, Quantum Inf. Process. **14** (2015), no. 3, 801–811. MR3312514
- [13] Samantha Pezzimenti and Abhinav Pandey, *Geography of Legendrian knot mosaics*, J. Knot Theory Ramifications **31** (2022), no. 1, Paper No. 2250002, 22. MR4411812
- [14] Eric J. Rawdon and Robert G. Scharein, *Using the HOMFLYPT polynomial to compute knot types*, Knotted Fields, 2024, pp. 319–342. MR4789615
- [15] Joshua M. Sabloff, *What is a Legendrian knot?*, Notices of the AMS **52** (2009), no. 10, 1282–1284.
- [16] The Sage Developers, *Sagemath, the Sage Mathematics Software System (Version 10.4)*, 2024. <https://doc-10-4--sagemath.netlify.app/html/en/reference/knots/sage/knots/link>.

A Calculation in Theorem 4

Here we provide the details of the calculation used to obtain the inequalities at the end of the proof of Theorem 4. The following Mathematica code computes the intersection of

$$V = \{(x_1, x_2, x_3, x_4, x_5) \in \mathbb{R}^5 : x_3 = x_4 = 0\}$$

with the image of $\mathbb{R}_{\geq 0}^{25}$ under the transformation $P : \mathbb{R}^{25} \rightarrow \mathbb{R}^5$. There are a few tricks used to make the calculation more manageable, including removing duplicate columns from the starting matrix P1, and using null space matrices to restrict the image to V .

```
P1={
  {0,0,-1/2,0,0,0,-1/2,0,0,0,-1,1,-1,-1,0,1,-1,-1},
  {0,0,1/2,0,0,0,-1/2,0,0,0,0,1,0,0,0,0,-1},
  {-1,-1,0,1,1,1,0,-1,0,-2,0,-2,0,0,2,2,0,0},
  {0,-1,-1,0,-1,1,1,1,0,0,-2,0,-2,0,0,0,2,2},
  {1,1,1,1,1,1,1,1,1,1,1,1,1,1,1,1,1,1,1,1}
};

E1={{0,0,1,0,0},{0,0,0,1,0}};
E2={{1,0,0,0,0},{0,1,0,0,0},{0,0,0,0,1}};

R1=Transpose[NullSpace[E1.P1]];
P2=E2.P1.R1;
R2=Transpose[NullSpace[P2]];

yVec=Transpose[{Array[y,Length[P2]]}];
vVec=Transpose[{Array[v,Length[R2[[1]]]}];

Q=Simplify[R1.(PseudoInverse[P2].yVec+R2.vVec)];
inequalities=Thread[Transpose[Q][[1]]>=0];

image=Reduce[Exists[{v[1],v[2],v[3],v[4],v[5],v[6],v[7],v[8],v[9],v[10],v[11],v[12],v[13]},inequalities],{y[1],y[2],y[3]}];
inequalities=Simplify[image/.{y[1]->tb,y[2]->rot,y[3]->n2}]
```

The output of this program gives a condition `inequalities` which constrains $P(\mathbb{R}_{\geq 0}^{25}) \cap V$ in terms of `tb`, `rot`, and `n2`. Here, `tb` represents $\text{tb}(\Lambda)$, `rot` represents $\text{rot}(\Lambda)$, and `n2` represents n^2 . For the rest of this calculation, to keep the notation from becoming unwieldy, we will write `tb` and `rot` to mean $\text{tb}(\Lambda)$ and

$\text{rot}(\Lambda)$ respectively. In this way, **inequalities** can be written as

$$\begin{aligned}
& (\text{tb} \leq 0 \wedge ((2 \text{rot} \leq \text{tb} \wedge 4 \text{rot} + n^2 \geq \text{tb}) \\
& \vee (\text{tb} < 2 \text{rot} \leq -\text{tb} \wedge \text{tb} + n^2 \geq 0) \\
& \vee (2 \text{rot} + \text{tb} > 0 \wedge n^2 \geq 4 \text{rot} + \text{tb}))) \\
& \vee ((4 \text{rot} + n^2 \geq \text{tb} \vee \text{rot} > 0) \wedge (n^2 \geq 4 \text{rot} + \text{tb} \vee \text{rot} \leq 0) \wedge \text{tb} > 0).
\end{aligned} \tag{*}$$

Mathematica is unable to simplify this statement any further, but it does have a simpler form. We claim that (*) is equivalent to the statement

$$(\text{tb} + n^2 \geq 0) \wedge (n^2 \geq 4|\text{rot}| + \text{tb}), \tag{†}$$

which we will show via the cases that follow. We will argue that in each case, the condition given by (*) is equivalent to (†).

Case (1.1) : $\text{tb} \leq 0$ and $2 \text{rot} \leq \text{tb}$.

We must show that $4 \text{rot} + n^2 \geq \text{tb}$ is equivalent to (†). Because $2 \text{rot} \leq \text{tb} \leq 0$, we know $|\text{rot}| = -\text{rot}$. So (†) can be written as

$$(\text{tb} + n^2 \geq 0) \wedge (n^2 \geq -4 \text{rot} + \text{tb}),$$

which is equivalent to

$$(\text{tb} + n^2 \geq 0) \wedge (4 \text{rot} + n^2 \geq \text{tb}).$$

The second inequality of this statement, $4 \text{rot} + n^2 \geq \text{tb}$, is the condition given in case (1.1). So we just need to show that case (1.1) also implies that $\text{tb} + n^2 \geq 0$. Combining $2 \text{rot} \leq \text{tb}$ and $4 \text{rot} + n^2 \geq \text{tb}$ tells us that $2 \text{tb} + n^2 \geq \text{tb}$. Rearranging this gives that $\text{tb} + n^2 \geq 0$. Therefore, (*) is equivalent to (†).

Case (1.2) : $\text{tb} \leq 0$ and $\text{tb} < 2 \text{rot} \leq -\text{tb}$.

In this case, the condition given by (*) is $\text{tb} + n^2 \geq 0$. The statement $\text{tb} + n^2 \geq 0$ is exactly the first half of (†), so we just need to show that we can also recover the second half, which states $n^2 \geq 4|\text{rot}| + \text{tb}$.

First consider if $\text{rot} \geq 0$. Because $2 \text{rot} \leq -\text{tb}$, we have $2 \text{rot} + \text{tb} \leq 0$. Multiplying by 2 gives $4 \text{rot} + 2 \text{tb} \leq 0$. We then have

$$\text{tb} + n^2 \geq 0 \geq 4 \text{rot} + 2 \text{tb}.$$

Since $\text{rot} \geq 0$, $|\text{rot}| = \text{rot}$, and thus, $\text{tb} + n^2 \geq 4|\text{rot}| + 2 \text{tb}$. Subtracting tb from both sides gives $n^2 \geq 4|\text{rot}| + \text{tb}$, as desired.

If $\text{rot} < 0$, we can make a similar argument using the fact that $\text{tb} < 2 \text{rot}$. We find that

$$2 \text{tb} - 4 \text{rot} < 0 \leq \text{tb} + n^2.$$

Subtracting tb from both sides then gives $n^2 \geq -4 \text{rot} + \text{tb}$. Since $\text{rot} < 0$, we have $|\text{rot}| = -\text{rot}$, and thus, $n^2 \geq 4|\text{rot}| + \text{tb}$. This completes case (1.2).

Case (1.3) : $tb \leq 0$ and $2\text{rot} > -tb$.

We must show that the statement $n^2 \geq 4\text{rot} + tb$ is equivalent to (\dagger) . In this case, our assumptions imply that $2\text{rot} > -tb \geq 0$. Thus, $\text{rot} > 0$, which means $|\text{rot}| = \text{rot}$. So the statement $n^2 \geq 4\text{rot} + tb$ is equivalent to $n^2 \geq 4|\text{rot}| + tb$, which is just the second part of (\dagger) . Thus, we just need to show that in this case, $n^2 \geq 4\text{rot} + tb$ implies the first part of (\dagger) , which is $tb + n^2 \geq 0$. Because $2\text{rot} > -tb$, we have $4\text{rot} + 2tb > 0$. Thus, we can subtract $4\text{rot} + 2tb$ from the right side of $n^2 \geq 4\text{rot} + tb$ to find that $n^2 \geq -tb$. Thus, $n^2 + tb \geq 0$, as desired.

In the remaining two cases, we want to show that if $tb > 0$, then the statement

$$(4\text{rot} + n^2 \geq tb \vee \text{rot} > 0) \wedge (n^2 \geq 4\text{rot} + tb \vee \text{rot} \leq 0) \quad (l)$$

is equivalent to (\dagger) . Note that exactly one of $\text{rot} > 0$ and $\text{rot} \leq 0$ will be true, so (l) can be rewritten as

$$(\text{rot} > 0 \wedge n^2 \geq 4\text{rot} + tb) \vee (\text{rot} \leq 0 \wedge 4\text{rot} + n^2 \geq tb). \quad (ll)$$

Case (2.1) : $tb > 0$ and $\text{rot} > 0$.

The condition given by (ll) in this case is $n^2 \geq 4\text{rot} + tb$, which we will show is equivalent to (\dagger) . Since $\text{rot} > 0$, $|\text{rot}| = \text{rot}$, so we have $n^2 \geq 4|\text{rot}| + tb$, which is the same as the second half of (\dagger) . It remains to show that this case also implies $tb + n^2 \geq 0$, which is true because both tb and n^2 are nonnegative.

Case (2.2) : $tb > 0$ and $\text{rot} < 0$.

The condition given by (ll) in this case is $n^2 + 4\text{rot} \geq tb$, which we will show is equivalent to (\dagger) . Since $\text{rot} \leq 0$, $|\text{rot}| = -\text{rot}$, and we obtain $n^2 \geq 4|\text{rot}| + tb$. Again, this is the same as the second half of (\dagger) , so it suffices to show that this case also implies $tb + n^2 \geq 0$. This is true because both tb and n^2 are nonnegative.

Since $(*)$ is equivalent to (\dagger) in every case, we have shown that they are equivalent conditions. Therefore, for any Legendrian knot Λ with a representation on an $n \times n$ mosaic, both of the following inequalities must be satisfied:

$$\begin{aligned} n^2 &\geq 4|\text{rot}(\Lambda)| + \text{tb}(\Lambda); \\ n^2 &\geq -\text{tb}(\Lambda). \end{aligned}$$

B Counting Legendrian Link Mosaics

Let $D_L^{(m,n)}$ be the number of $m \times n$ Legendrian link mosaics. The following is an implementation in Mathematica of the algorithm given in Section 4 to compute $D_L^{(m,n)}$:

```
x[0] = o[0] = {{1}};
x[n_] := ArrayFlatten[{{x[n - 1], o[n - 1]}, {o[n - 1], x[n - 1]}}];
o[n_] := ArrayFlatten[{{o[n - 1], x[n - 1]}, {x[n - 1], 3 * o[n - 1]}}];
legendrian[m_, n_] :=
  If[m > 1 && n > 1,
    2 * Total[MatrixPower[x[m - 2] + o[m - 2], n - 2],
      2], 1];
ParallelTable[legendrian[m, n], {m, 1, 11}, {n, 1, m}]
```

Tables B.1, B.2, and B.3 below list all values of $D_L^{(m,n)}$ for $1 \leq n \leq m \leq 11$.

	$D_L^{(11,n)}$
$n = 1$	1
$n = 2$	1,024
$n = 3$	11,208,704
$n = 4$	236,710,854,656
$n = 5$	6,252,734,836,998,144
$n = 6$	181,637,396,577,778,663,424
$n = 7$	5,528,978,020,972,513,728,659,456
$n = 8$	172,538,354,498,746,094,406,296,666,112
$n = 9$	5,458,581,384,707,531,006,284,534,386,786,304
$n = 10$	174,020,259,805,998,593,378,475,801,984,133,758,976
$n = 11$	5,571,666,891,811,926,168,753,521,842,383,673,521,864,704

Table B.1: The numbers $D_L^{(11,n)}$ of $11 \times n$ Legendrian link mosaics, $1 \leq n \leq 11$.

$D_T^{(m,n)}$	$m = 3$	$m = 4$	$m = 5$	$m = 6$	$m = 7$	$m = 8$
$n = 1$	1	1	1	1	1	1
$n = 2$	4	8	16	32	64	128
$n = 3$	20	104	544	2,848	14,912	78,080
$n = 4$		1,504	22,208	329,216	4,883,968	72,464,384
$n = 5$			948,032	40,930,304	1,772,261,888	76,795,762,688
$n = 6$				5,204,262,912	666,548,862,976	85,575,149,027,328
$n = 7$					254,112,496,082,944	97,392,800,416,399,360
$n = 8$						111,879,597,850,371,293,184

Table B.2: $D_L^{(m,n)}$ for all $1 \leq n \leq m \leq 8$, omitting $D_L^{(1,1)} = D_L^{(2,1)} = 1$ and $D_L^{(2,2)} = 2$.

$D_L^{(m,n)}$	$m = 9$	$m = 10$
$n = 1$	1	1
$n = 2$	256	512
$n = 3$	408,832	2,140,672
$n = 4$	1,075,195,904	15,953,379,328
$n = 5$	3,328,369,229,824	144,260,644,012,032
$n = 6$	10,995,378,691,637,248	1,413,150,484,120,731,648
$n = 7$	37,406,060,364,420,743,168	14,378,743,075,001,419,694,080
$n = 8$	129,059,960,656,754,513,018,880	149,160,169,737,929,856,250,806,272
$n = 9$	448,381,477,417,976,615,986,528,256	1,563,124,967,138,785,231,707,530,330,112
$n = 10$		16,469,260,582,635,747,355,818,375,736,459,264

Table B.3: $D_L^{(m,n)}$ for all $9 \leq m \leq 10$ and $1 \leq n \leq m$.

C Census Diagrams

In this section, we provide censuses of known mosaic numbers of Legendrian knots. Recall that for any smooth knot type, its Legendrian representatives can be depicted in a mountain range organized by their classical invariants. We label each Legendrian representative in each mountain range with its mosaic number or our best bounds on it (indicated with a “ \geq ” symbol), as determined by the computer search described in Section 5, the bounds given in Sections 2 and 3, and our own constructions. Yellow vertices denote examples of representatives where stabilization decreases the mosaic number. As the sign of a Legendrian knot’s rotation number depends only on its orientation, the censuses presented in this paper include only the right half of the mountain diagram where knots have non-negative rotation number. A complete census can be obtained by mirroring these censuses horizontally about the column with $\text{rot} = 0$.

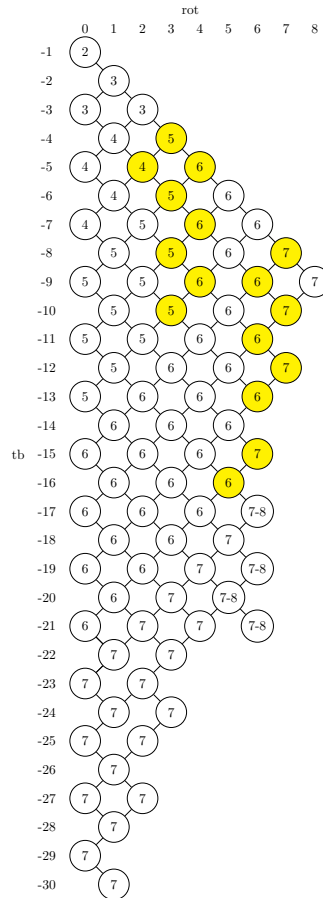


Figure C.1: Unknot census

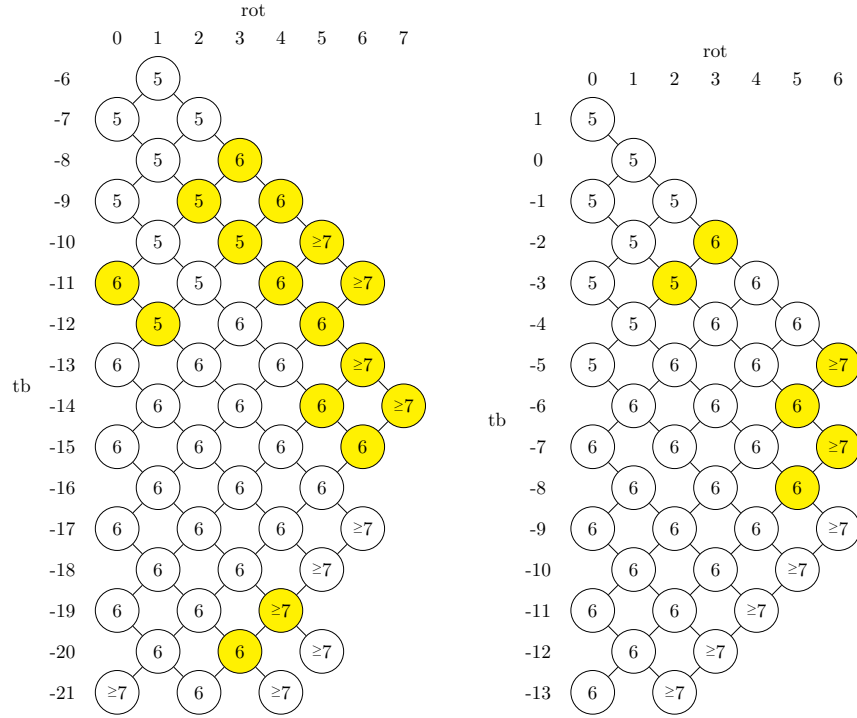


Figure C.2: Negative (i.e., 3_1) and positive (i.e., $m(3_1)$) trefoil censuses

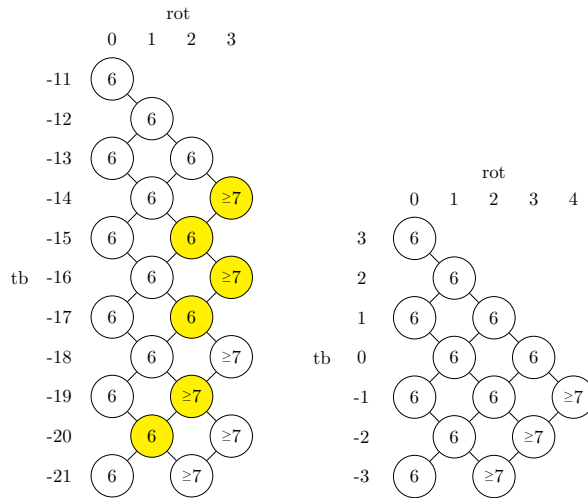


Figure C.3: Negative (i.e., $3_1\#3_1$) and positive (i.e., $m(3_1)\#m(3_1)$) granny knot censuses

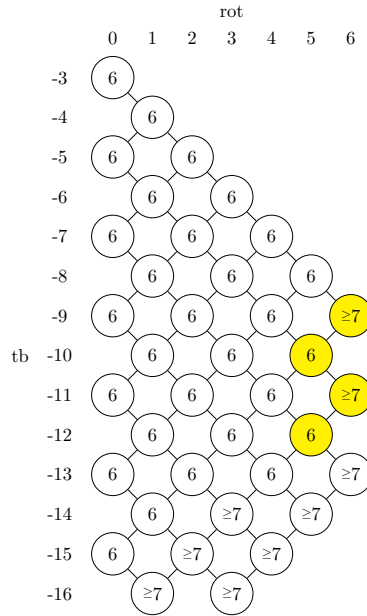


Figure C.4: $4_1 = m(4_1)$ census

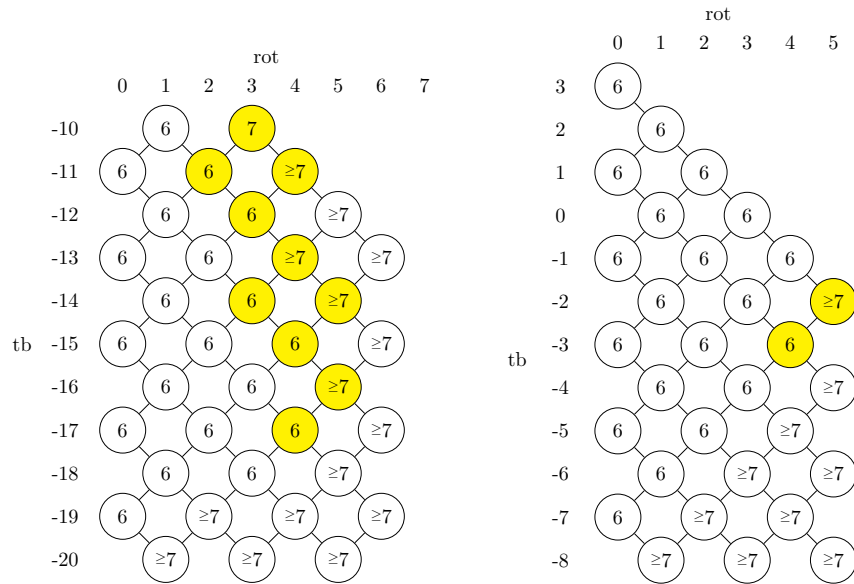


Figure C.5: 5_1 and $m(5_1)$ censuses

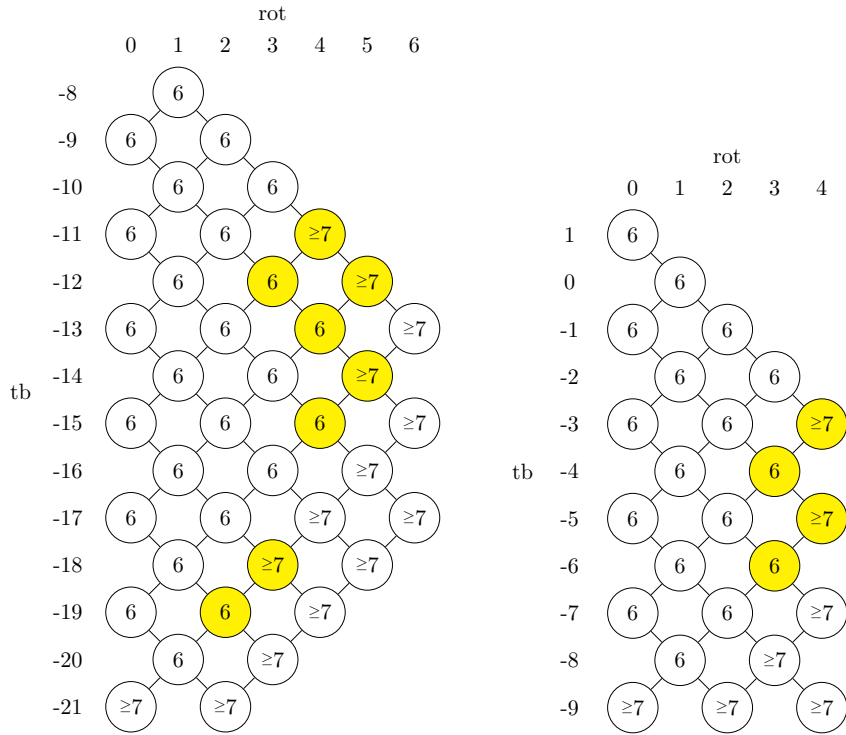


Figure C.6: 5_2 and $m(5_2)$ censuses

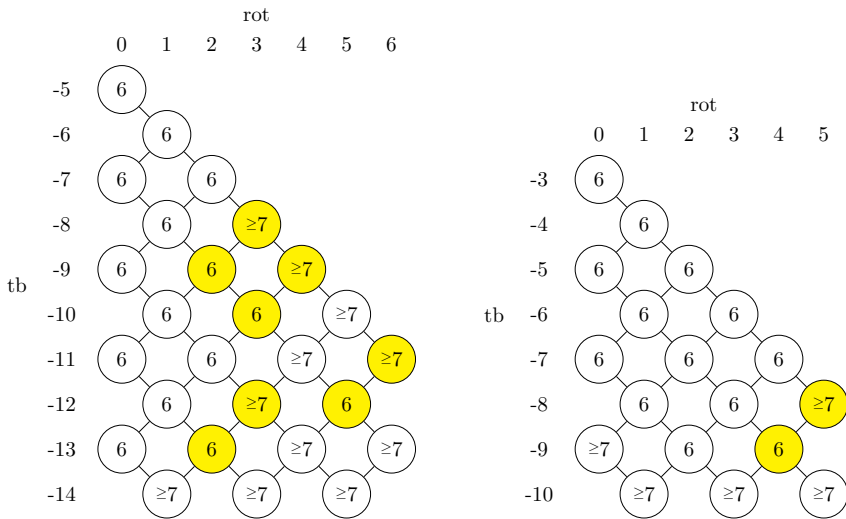


Figure C.7: 6_1 and $m(6_1)$ censuses

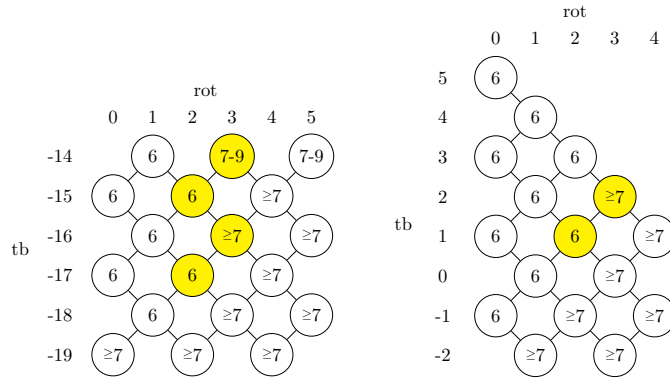


Figure C.8: 7_1 and $m(7_1)$ censuses

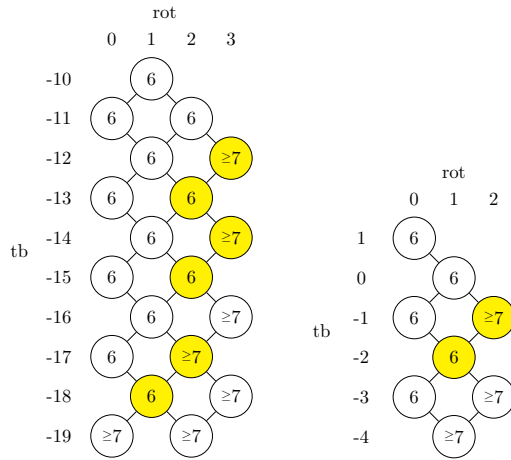


Figure C.9: 7_2 and $m(7_2)$ censuses

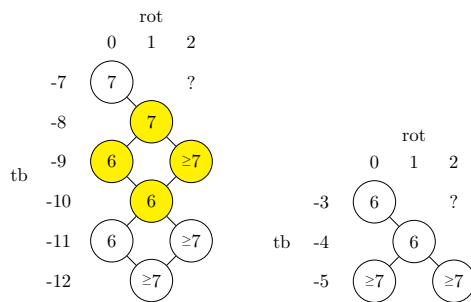


Figure C.10: 8_1 and $m(8_1)$ censuses

D Minimal Mosaics

In this section, we provide computationally derived mosaics demonstrating the upper bounds shown in Appendix C. The mosaics listed are of the minimal size necessary to depict their respective Legendrian knots, and follow the format established in Section 5.2. These mosaics can be converted into images using the python program `to_image.py`, which can be found at [10].

Table D.1: Minimal Mosaics for Legendrian knots Λ with $m(\Lambda) \leq 6$.

tb	rot	Minimal Mosaic
0_1		
-1	0	2134
-2	1	021246354
-3	0	021284340
-3	2	0021024624063554
-4	1	0000021028913434
-4	3	000210024602406240635554
-5	0	0021028428403400
-5	2	0210279139840340
-5	4	0212128746399162434635554
-6	1	0021028428913434
-6	3	0002100246028162439435540
-6	5	00000025551062128138984624340635554
-7	0	2121398428913434
-7	2	0000000210027912898434340
-7	4	00000000021021246279916398846034354
-7	6	00212102874628460639591624034635554
-8	1	0000000210028812898434340
-8	3	0021002791279843984003400
-8	5	000021000246002816028466243594355540
-9	0	0000002121288843989103434
-9	2	0002100284027912898434340
-9	4	000000000210002871028794243991355434
-9	6	00212102874628791639984624340635554
-10	1	0002100284028812898434340
-10	3	0212127984399712878434340
-10	5	000021000246002816028794243991355434
-11	0	0002121284398812898434340
-11	2	0212127984398712888434340
-11	4	000000002121027984279971398784034340
-11	6	002121028746287954379951246624354340
-12	1	0212127984398812898434340
-12	3	000000002121027984279871398884034340
-12	5	000021021246287816379794289791343434
-13	0	0212128884398812898434340
-13	2	000000002121027984279881398984034340
-13	4	000021021246279916398884288891343434
-13	6	021210287791379984279971398984034340
-14	1	000000000210212881398884289891343434
-14	3	000021021246279716398884289891343434
-14	5	002121027984279971399784287840343400
-15	0	000000002121028884288881398984034340
-15	2	0000000021210279881398884289891343434
-15	4	002121027984279871398894288891343434
-16	1	0000000021210288881398884289891343434
-16	3	000251021624279881398884289891343434
-16	5	212121398846288816398794243991355434
-17	0	000021021284287881388884289891343434
-17	2	000021021284279881398884289891343434
-17	4	212121397984297881638884629891343434
-18	1	000021021284288881398884289891343434
-18	3	002121027984279881398884289891343434
-19	0	002121028784288881388884289891343434
-19	2	002121027984288881398884289891343434
-20	1	002121028884288881398884289891343434
-21	0	212121398884288881398884289891343434
3_1		
-6	1	0021002971294663759403540
-7	0	0021002971298463791603434
-7	2	02100289103997103794000340
-8	1	0021002871298943794000340
-8	3	000000002100029710243991355984000340
tb	rot	Minimal Mosaic
-9	0	0021002971298843799103434
-9	2	0021002871298943799103434
-9	4	000210002460029160243991355984000340
-10	1	0021025891629843989103434
-10	3	0021002891289843984003400
-11	0	000000000210002971029884287991343434
-11	2	0021002891289843989103434
-11	4	000000002100028710288991379984034340
-12	1	2121039891289843989103434
-12	3	000000000210002891028984289840343400
-12	5	000210002460028160288991379984034340
-13	0	000000002121029784298881379984034340
-13	2	000000000210002891028984289891343434
-13	4	000000002121028784288991379984034340
-14	1	000000000210212891398984289891343434
-14	3	000000002121028984289871398884034340
-14	5	000210002791028984289971398784034340
-15	0	000000021210279891398984289891343434
-15	2	000000002121028984289881398984034340
-15	4	00002102128428789137998428984034340
-15	6	021210287791379984289971398784034340
-16	1	000000021210288891398984289891343434
-16	3	000021021284287891379984289891343434
-16	5	00212102798428997139988428784034340
-17	0	000021021284279891398984289891343434
-17	2	000021021284287891388984289891343434
-17	4	002121027984289971399884287891343434
-18	1	00002102128428891398984289891343434
-18	3	002100028910289881398884289891343434
-19	0	00212102798428891398984289891343434
-19	2	002121028784288891388984289891343434
-20	1	002121028884288891398984289891343434
-21	2	212121398884288891398984289891343434
$m(3_1)$		
1	0	0021025971629943943103554
0	1	0021002891299463791603434
-1	0	0021002891299843794003400
-1	2	021002891039791243463554
-2	1	0021002891299843799103434
-2	3	000000002100028910284391395546035554
-3	0	0210028710397912898434340
-3	2	0212128946397162894634354
-3	4	00000002121028989139746624354635554
-4	1	0212128784397912894634354
-4	3	000000002121028946289716397946034354
-4	5	002121028946299916639746628406343554
-5	0	0212128784397912898434340
-5	2	000000000210212891399984287991343434
-5	4	000021021246289816397466289546343554
-6	1	000000002121028784279791398984034340
-6	3	0000000212102898913979742438991355434
-6	5	002121259746628816639794627991343434
-7	0	000000002121028784288791398984034340
-7	2	000000021210287891397974289891343434
-7	4	000210212791399984279791398984034340
-8	1	000000021210287881397984289891343434
-8	3	00002102124628981639794289891343434
-8	5	021210279791399984279791398984034340
-9	0	000021021284287791397984289891343434
-9	2	000021021246289816397884289891343434
-9	4	002121028946288916397994289891343434
-10	1	000021021284287881397984289891343434
-10	3	002121028784287991397974289891343434
-11	0	002121027984287881397984289891343434
-11	2	002121028784287981397984289891343434
-12	1	002121028784288791398884289891343434
-13	0	212121398784288791398884289891343434

tb	rot	Minimal Mosaic
$3_1 \# 3_1$		
-11	0	255100602910629891398946039406003554
-12	1	002100258910629891398946039406003554
-13	0	002100258910629891398946039424003540
-13	2	002100028910289891398946039406003554
-14	1	002100028910289891398946039424003540
-15	0	002100028910289891398984039840003400
-15	2	002100028910289891398946289406343554
-16	1	002100028910289891398946289424343540
-17	0	002100028910289891398984289840343400
-17	2	002121028984289891398946289406343554
-18	1	0021000289102898913989842898913434340
-19	0	002121028984289891398984289840343400
-20	1	0021210289842898913989842898913434340
-21	0	2121213989842898913989842898913434340
$m(3_1) \# m(3_1)$		
3	0	002100029710297971379794037940003400
2	1	002100029710297971379794037991003434
1	0	002100029710297971379794243991355434
1	2	002100029710297971639794627991343434
0	1	002100029710297971379794287991343434
0	3	002551029124297971639794627991343434
-1	0	002121029746297916379794287991343434
-1	2	002121029784297971639794627991343434
-2	1	002121029784297971379794287991343434
-3	0	212121399784297971379794287991343434
4_1		
-3	0	000000021210297971379466037594003540
-4	1	000000002100028910299971379794034340
-5	0	000000002100028710298971379794034340
-5	2	000000002100028910289791394346035554
-6	1	000000002100028710289791398946034354
-6	3	00000000210002971028991398984034340
-7	0	00000000210002891028979139894034340
-7	2	000000002100028710289791398984034340
-7	4	00000000255102912428991398984034340
-8	1	000000002121028784289791398946034354
-8	3	00000000212102978428991398984034340
-8	5	000010212891399984063991062984034340
-9	0	000000002121028984289791398784034340
-9	2	000000002121028784289791398984034340
-9	4	000021021284289891399984243940355400
-10	1	0000000021210287891397984289891343434
-10	3	000021021284289891399984243991355434
-10	5	0000210212891399984277991398984034340
-11	0	000021021284287891397984289840343400
-11	2	000021021284289891377984289840343400
-11	4	000210212891399984287991388984034340
-11	6	0021210289791399984289991398984034340
-12	1	000021021284287891397984289891343434
-12	3	002121027984289891377984289840343400
-12	5	0021210288891399984277991398984034340
-13	0	002121027984287891397984289891343434
-13	2	002121027984289891377984289891343434
-13	4	0021210288891399984287991388984034340
-14	1	002121028784288791398984289891343434
-14	3	002121028784288791398984289891343434
-15	0	212121398784288791398984289891343434
5_1		
-10	1	000000002100029710298991379946034354
-11	0	000000002551029124298991379946034354
-11	2	000000002100029710298991379984034340
-12	1	000000002121029784298991379946034354
-12	3	000210002460029160298991379984034340
-13	0	0000000021210289971399894243991355434
-13	2	000000002121029784298991379984034340
-14	1	0000000021210289971399894287991343434
-14	3	000210002871028894298991379946034354
-15	0	000021021246289916399894287991343434
-15	2	000021021284289971399894287940343400
-15	4	000210002871028894298991379984034340
-16	1	000021021284289971399894287991343434
-16	3	000210212871398894298991379984034340
-17	0	002121028846289916399894287991343434
-17	2	002121027984289971399894287991343434
-17	4	021210287871388894298991379984034340
-18	1	002121028884289971399894287991343434
-18	3	021210288871398894298991379984034340
-19	0	212121398884289971399894287991343434
$m(5_1)$		
3	0	000000025100062910299791379946034354
2	1	000000002100028910299791379946034354
1	0	000000002100028910299791379984034340
1	2	000021251246629916397994039840003400
0	1	000000002121028984299791379946034354
0	3	000210255971625994662791398984034340

tb	rot	Minimal Mosaic
-1	0	000000002121028984299791379984034340
-1	2	000021251246629916397994289840343400
-1	4	021210289791397994284391395546035554
-2	1	0000000021210289971397994289891343434
-2	3	002121028984299791639946628406343554
-3	0	000021021246289916397994289891343434
-3	2	000210212791398984299791379984034340
-3	4	021210289891397466289166397946034354
-4	1	000021021284289971397994289891343434
-4	3	021210279791398984299791379984034340
-5	0	002121028846289916397994289891343434
-5	2	002121027984289971397994289891343434
-6	1	002121028884289971397994289891343434
-7	0	021210287881397984288791398984034340
5_2		
-8	1	000210025971062994299971379794034340
-9	0	000000251210629891397946039406003554
-9	2	002100028910299971379794037940003400
-10	1	000000002100258910629791398984034354
-10	3	002100028910299971639794627940343400
-11	0	000000002100258910629791398984034340
-11	2	000000002100028910289791398984034354
-12	1	000000002100028910289791398984034340
-12	3	000210002891028984299771379984034340
-13	0	000000002121258984629791398984034340
-13	2	000000002121028984289791398984034354
-13	4	021210287891379984299771379984034340
-14	1	000000002121028984289791398984034340
-14	3	000210002791028984289791398984034354
-15	0	0000000021210289891397984289891343434
-15	2	000021251284629891397984289840343400
-15	4	021210287791379984289791398984034354
-16	1	000021021284289891397984289840343400
-16	3	002121028984289791398846289406343554
-17	0	000021021284289891397984289891343434
-17	2	002100028910289791398884289891343434
-18	1	002121027984289891397984289891343434
-19	0	002121028884289891397984289891343434
-19	2	002121028984289791398884289891343434
-20	1	212121398884289891397984289891343434
$m(5_2)$		
1	0	000000002100029710298971379794034340
0	1	000000002121029746298916379794034340
-1	0	000000002121029784298971379794034340
-1	2	0000000021210297971639894627991343434
-2	1	0000000021210297971379894287991343434
-2	3	000210212891399946298916379846034354
-3	0	000021021246297916379894287991343434
-3	2	000021021284297971639894627991343434
-4	1	000021021284297971379894287991343434
-4	3	002121027984297971639894627991343434
-5	0	000210212891399984288991379984034340
-5	2	000210212871399894289991398984034340
-6	1	002121028884297971379894287991343434
-6	3	021210279891398984298991379984034340
-7	0	002121028984297791379984289891343434
-7	2	002121028984289791399784287991343434
-8	1	212121398984289791399784287991343434
6_1		
-5	0	021000297100379910299791379946034354
-6	1	000210255971602994629791398946034354
-7	0	000210002971258994629791398946034354
-7	2	021000289121397946299916379794034340
-8	1	000210002891028984299791379946034354
-9	0	000210212891398984299791379946034354
-9	2	000210002891028984299791379984034340
-10	1	000210212891398984299791379984034340
-10	3	021210287891379984299791379984034340
-11	0	021000287121397984289791398984034340
-11	2	021000289121377984289791398984034340
-12	1	021210287791397984289791398984034340
-13	0	021210287881397984289791398984034340
-13	2	021210287891397984288791398984034340
$m(6_1)$		
-3	0	000210025971295894662971379794034340
-4	1	000210002971029846298916379794034340
-5	0	000210002871029894298971379794034340
-5	2	000210002891029984298991379946034354
-6	1	000210212871399894298971379794034340
-6	3	000210002891029984298991379984034340
-7	0	021210279871398984298971379794034340
-7	2	000210212971398984289991398984034340
-8	1	000210212891399984298991379984034340
-8	3	021210279891399984298991379984034340

tb	rot	Minimal Mosaic
-9	2	021210288971399894298991398984034340
-9	4	021210288891399984298991379984034340
$\bar{7}_1$		
-14	1	000210002971029894298991379946034354
-15	0	000210212971399894298991379946034354
-15	2	000210002971029894298991379984034340
-16	1	000210212971399894298991379984034340
-17	0	021210279971399894298991379984034340
-17	2	021210287971389894298991379984034340
-18	1	021210288971399894298991379984034340
$m(\bar{7}_1)$		
5	0	021210299971397994299791379946034354
4	1	021000289100397910299791379946034354
3	0	021000289100397910299791379984034340
3	2	021210289791397994299791379946034354
2	1	021000289121397984299791379946034354
1	0	021000289121397984299791379984034340
1	2	021210289891397974299791379946034354
0	1	021210289791397984299791379984034340
-1	0	021210289881397984299791379984034340
$\bar{7}_2$		
-10	1	021210297971379994299791379946034354
-11	0	251210629891397946299716379946034354
-11	2	021210289971397994299971379794034340
-12	1	021210289891397946299716379946034354
-13	0	021000289100397910289791398946034354
-13	2	021210287891397984299791379946034354
-14	1	021000289100397910289791398984034340
-15	0	021000289121397984289791398946034354
-15	2	021210289791397994289791398984034340
-16	1	021000289121397984289791398984034340
-17	0	021210289791397984289791398984034340
-18	1	021210289881397984289791398984034340
$m(\bar{7}_2)$		
1	0	000210002971029894298971379794034340
0	1	000210212971399894298971379794034340
-1	0	021210279971399894298971379794034340
-2	1	021210288971399894298971379794034340
-3	0	021210289891399984298991379984034340
$\bar{8}_1$		
-9	0	251210629891397984299791379946034354
-10	1	021210289891397984299791379946034354
-11	0	021210289891397984299791379984034340
$m(\bar{8}_1)$		
-3	0	021210297971379894298991379946034354
-4	1	021210289971399894298971379794034340